

# Geometric design parameterization and optimization of spar floating offshore wind turbine substructure

Ojo, Adebayo; Collu, Maurizio; Coraddu, Andrea

DOI

10.1016/j.oceaneng.2025.121378

**Publication date** 

**Document Version** Final published version

Published in Ocean Engineering

Citation (APA)
Ojo, A., Collu, M., & Coraddu, A. (2025). Geometric design parameterization and optimization of spar floating offshore wind turbine substructure. Ocean Engineering, 332, Article 121378. https://doi.org/10.1016/j.oceaneng.2025.121378

Important note

To cite this publication, please use the final published version (if applicable). Please check the document version above.

Copyright

Other than for strictly personal use, it is not permitted to download, forward or distribute the text or part of it, without the consent of the author(s) and/or copyright holder(s), unless the work is under an open content license such as Creative Commons.

Please contact us and provide details if you believe this document breaches copyrights. We will remove access to the work immediately and investigate your claim.

ELSEVIER

Contents lists available at ScienceDirect

# Ocean Engineering

journal homepage: www.elsevier.com/locate/oceaneng



## Research paper

# Geometric design parameterization and optimization of spar floating offshore wind turbine substructure

Adebayo Ojo <sup>a</sup>, Maurizio Collu <sup>a,\*</sup>, Andrea Coraddu <sup>b</sup>

#### ARTICLE INFO

Keywords: FOWT MDAO Parameterization Substructures Optimizers

#### ABSTRACT

The push to attain commercialization of the floating offshore wind industry and subsequently achieving net-zero carbon emission by the year 2050 requires the utilization of cutting-edge design and analyses techniques. Geometric design parameterization and optimization is an effective technique that can be employed in modelling and optimizing a Floating Offshore Wind Turbine (FOWT) substructure. It is an essential framework with the capability of innovative concept generation of platform types in the FEED design phase.

This study addresses the conceptual design shape generation, multidisciplinary design analysis and optimization (MDAO) of spar variants FOWT substructure developed from the standard NREL OC3 spar. The methodology involves the use of non-uniform rational basis spline (NURBS) parameterization technique to generate design variants with the flexibility of varying the control points to facilitate varying geometric shapes due to the local propagation property of the NURBS curve. Design variables passed through the NURBS curves control points generates a robust and rich design space and the potential flow hydrodynamic analysis tool in the DNV SESAM suite is used to estimate the hydrodynamic response. The design and analysis phases are explored and exploited for optimal design solution based on specified objectives and constraints with the use of state-of-the-art derivative-free optimizers. The optimal designs were evaluated for three sets of FOWT static pitch angle constraints (5, 7 and 10) degrees, a positive ballast constraint for stability and a constraint on nacelle acceleration root mean square (RMS) value below 30 % of the gravitational acceleration. The single objective function considered in the study is to ensure a minimum mass of the steel material utilized in the design, which invariably leads to a reduction in cost of the substructure material used in fabrication. Achieving this single objective results in an altered geometric shape variants from the baseline OC3 spar substructure for all the three cases evaluated.

Verification of the nacelle acceleration response in time domain was further evaluated for the three optimal design cases selected and compared with recommended standards which is below 0.3 g. Although, the nacelle acceleration for the optimal variants is more conservative in time domain assessment than the frequency domain assessment, the values are still below the recommended 0.3 g from standards. Also, the masses of selected optimal design for each constraint were compared to the standard OC3 case study. An observation made in this study is that as the static pitch angle of the FOWT system gets larger, the lower the mass of the optimal substructure and inherently the capital expenditure of the substructure. Finally, the selected optimized platforms were analysed with a non-linear, time domain approach to confirm the level of accuracy of the key response parameters obtained with the frequency-based approach.

Abbreviations  AHSE Aero-Hydro-Servo-Elastic		(continued)	
		Abbreviations	
B-Spline	Basis Spline	DLC	Design Load Case
CAPEX	Capital Expenditure	DOF	Degree of Freedom
DNV	Det Norske Veritas	ELM	Extreme Learning Machines
	(continued on n	ext column)	(continued on next page)

<sup>\*</sup> Corresponding author.

E-mail addresses: adebayo.ojo@strath.ac.uk (A. Ojo), maurizio.collu@strath.ac.uk (M. Collu), a.coraddu@tudelft.nl (A. Coraddu).

https://doi.org/10.1016/j.oceaneng.2025.121378

<sup>&</sup>lt;sup>a</sup> Department of Naval Architecture Ocean and Marine Engineering, University of Strathclyde, Glasgow, G4 OLZ, UK

b Department of Maritime & Transport Technology, Delft University of Technology, 2628 CD, Delft, the Netherlands

#### (continued)

Abbreviations	
FEM	Finite Element Method
FFD	Free Form Deformation
FOWF	Floating Offshore Wind Farm
FOWT	Floating Offshore Wind Turbine
FVAWT	Floating Vertical Axis Wind Turbines
GB	Gradient Based
GF	Gradient Free
HAWT	Horizontal Axis Wind Turbine
HF	High Fidelity
IEC	International Electrotechnical Commission
JONSWAP	Joint North Sea Wave Project
LCOE	Levelized Cost Of Energy
MDA	Multidisciplinary Design Analysis
MDAO	Multidisciplinary Design Analysis and Optimization
NURBS	Non-Uniform Rational B-Spline
OC3	Offshore Code Comparison Collaboration
OWT	Offshore Wind Turbine
PSM	Pattern Search Model
RAO	Response Amplitude Operator
RMS	Root Mean Square
RNA	Rotor Nacelle Assembly
TLP	Tension-Leg Platform
WADAM	Wave Analysis by Diffraction and Morison Theory
WAMIT	Wave Analysis at Massachusetts Institute of Technology

#### 1. Introduction

#### 1.1. Background

The urgent need for clean energy is quite imperative to halt climate change. The technology of floating offshore wind turbine is one that can facilitate this change to clean energy with its capability to access richer wind resources in deep waters (water depth exceeding 60 m). The main design concepts of FOWT substructures are the spar, the semisubmersible, and the tension-leg Platform (TLP), that have been tried and tested in the offshore hydrocarbon sector. However, in the FOWT sector, the floating substructure represents a significant part of the capital expenditure (CAPEX) of the system as highlighted by Ioannou et al. (2020), in which 29 % of the FOWT system's CAPEX is spent on the floating substructure in comparison to 13.5 % of the CAPEX spent on a bottom fixed wind turbine's foundation. To speed up the increase in use of floating technology, there is need to reduce the floating foundation cost in comparison to the fixed foundation. Also, apart from the capital cost reduction, the computational cost of the design and analysis in time is also essential. This leads to the need of bespoke geometric designs with adequate shape modification approach integrated within a multidisciplinary design analysis and optimization (MDAO) framework as detailed in Ojo et al. (2022a).

The platform he considered is of the spar type. Although the spar concept is one of the most mature, convenient for mass production and certification as a result of its simple geometry, it is still being advanced with innovative designs to unlock its potential, amongst which are: improved system's motion performance, simplified handling (construction, assembly, transportation and installation), and reduction in cost (Leimeister et al., 2018). Some advanced work conducted on the spar platform is highlighted in this section.

Advanced spar type substructure for a floating substation (Fukushima Kizuna) used in the FOWF's Demonstration (Project FORWARD) in Fukushima consists of a spar platform with columns at the upper, middle, and bottom ends. This structure improves motion performance, allows utilization in around 110 m water depth and lowers installation costs (Leimeister et al., 2022; Wright et al., 2019; Yoshimoto and Kamizawa, 2019). To shorten the total length of the spar and lower the cost of the system, Hirai et al. (2018) and Yamanaka et al. (2017) both employ a tri-segmented shaped spar-buoy with a bigger diameter section

in the center. However, Zhu et al. (2019) reversed the configuration by placing the smaller diameter cylinder in the middle segment, with a focus on enhancing motion performance and increasing restoring capabilities.

An innovative enhancement in stability is highlighted in the Massachusetts Institute of Technology's innovative spar-type floater, with a relatively shallow draft and stabilised by a two-layer taut-leg mooring system (Butterfield et al., 2007). Additionally, the common spar floater can be advanced by an extra adjusted damper on the system's mass (He et al., 2019) or the addition of a moon pool (Pham and Shin, 2019).

Other innovations are borrowed from the oil and gas sector and found in designs like the truss spar platforms. In these designs, a truss section connects a bottom tank to the floating platform, with heave plates or helical strakes added to enhance the dynamic response (Leimeister et al., 2022).

A comprehensive parametric analysis of a FOWT is detailed in Tracy (2007), where the optimization process led to the development of Pareto fronts, comparing the turbine RMS - root mean square acceleration with various objectives for offshore structures. Essentially, this analysis highlights the objective's trade-offs (system's performance, cost), identifying structure displacement and total mooring line tension as the two primary factors influencing costs.

From a material point of view Sandner et al. (2014) propose a concrete spar platform in the form of a torus with various sizes that may support the InnWind EU 10 MW reference wind turbine. According to the potential flow calculations used in the study, the response to wave excitation is quite low for all evaluated geometries in comparison to a typical wave spectrum. Every shape has a distinct surge, heave, and pitch RAO (Response Amplitude Operator) peak for very low frequencies. The size of these distinct peaks is planned to be reduced as discussed in the study with dampening plates at the structure's keel. The mooring system for this kind of platform will need to be thoroughly designed to avoid the low-frequency excitation due to slow drift forces (Sandner et al., 2014).

Early studies that have applied an optimization framework to enhance the hydrodynamic response of oil and gas' floaters are detailed in Birk (2006); Clauss and Birk (1996) and this knowledge is being adopted in the FOWT sector. Although FOWT system is still in the pre-commercial stage, there is now a lot of interest in the technology allowing a flurry of optimization studies to be conducted in advancing the design of the system. Optimization studies that detail the cost reduction and enhancing the hydrodynamic response of FOWT systems are highlighted in Fylling and Berthelsen (2011); Hall et al. (2013); Karimi (2018); Karimi et al. (2019); Karimi et al. (2017); Sandner et al. (2014).

The examples of innovative work highlighted here are all based on a cylindrical spar design, with the design variables for alteration limited to the diameter of the cylindrical spar and the draft. A change in this approach is highlighted in Ojo et al. (2022b), where the authors have used the FEDORA framework developed within the University of Strathclyde with commercial software from the DNV Manager suite (SESAM Genie and HydroD/WADAM) to parameterize and optimize the geometry of a 5 MW OC3 spar.

#### 1.2. Aim, objective and contribution to knowledge

The main aim is to explore innovative geometrical shapes for a spar configuration, integrating this design concept into a state-of-the-art MDAO framework to search, and identify an optimal design from a rich design space. Key objectives of this study are highlighted herein:

 Minimize the structural steel mass required for the spar-type support structure design, hence, reducing the material cost, weight and potential environmental impact.

- Investigate innovative geometric configurations for spar-type floating substructure that meets the stability and hydrodynamic design requirements.
- Apply advanced shape parametric techniques that allow for flexible and precise geometric modelling within the optimization process.

Achieving these objectives requires the use of optimization algorithm and parametric design techniques to explore and exploit the design space. Unlocking the optimal geometric shape design for spar floaters within the MDAO framework necessitates a solid grasp of shape parametric design techniques, which are effectively utilized in multidisciplinary fields such as aerospace, automotive, and oil and gas industries. These advanced parameterization methods have been thoroughly detailed in the work of Samareh (2001) and include the splines technique like B-Spline and Non-Uniform Rational B-Spline (NURBS). The NURBS method represents a cutting-edge parametric approach that enables geometric modifications by adjusting control points along the design plane.

The contribution to knowledge of this study is investigating the effectiveness of the MDAO framework that uses parametric free-form curves, and demonstrating that novel, innovative geometry shapes can be found, which not only satisfy the constraints imposed, but also lower the mass of structural steel; eventually facilitating the total capital cost's reduction. This study developed a glue code for automating the design and calculating the accurate ballast required for the compartment model to ensure hydrostatic stability of the FOWT system within the exploration phase of the MDAO framework. The study also developed codes to interface the multiple disciplines (aero-hydro-servo-elasto disciplines) within the framework.

#### 1.3. Limitation of study

The ability of lowering the capital cost is very beneficial since the capital cost of floating foundation far exceeds the capital cost of fixed foundation as highlighted in (Ioannou et al., 2020; Tyler and Patrick, 2022). However, it is imperative to highlight a potential limitation of this study which is the manufacturability of the bespoke geometric shape of the floaters. The complexity of manufacturing the selected bespoke shaped designs when considered has the potential to drive up the capital cost as traditional metalworking processes quite often involve a significant amount of material waste, as reported by ElMaraghy et al. (2012). To minimize material waste which leads to high costs, the concept of additive manufacturing could be explored. This is an ongoing area of research that could potentially reduce the manufacturing complexity costs of bespoke geometric shapes. As highlighted in Gardner (2023), metal additive manufacturing (Direct energy deposition and Wire-arc additive manufacturing) or 3D printing is still in its infancy, it has now reached a scale appropriate for construction use, offering the potential for enhanced cost-effectiveness, sustainability, safety, and productivity through increased automation, better customization, and reduced material consumption and waste (Gardner, 2023). However, comparing additive manufacturing with subtractive manufacturing, the additive manufacturing components tend to have inferior surface finishing and accuracy of dimension as it is an ongoing research area for the future (Qiu et al., 2022).

#### 1.4. Structure of study

The structure of this work is as follows: Section 1 provides an introductory overview and it also details the aim and objectives of the study while highlighting the limitation of the study framework. Section 2 highlights the methodology of the geometry design analysis and optimization framework utilized in this work. It also details state-of-the-art design, analysis and optimization process of a FOWT Spar platform with an introduction to parameterization techniques within an MDAO framework, to further advance the optimization process of the spar-buoy

floater. Section 3 highlights the conventional modelling and analysis technique of an OC3 FOWT spar in frequency domain using the potential flow theory and also coupling the platform design to the reference turbine system in OpenFAST – a medium fidelity time domain simulation tool for verification of the potential flow tool. Section 4 details the application of the innovative MDAO framework detailed in Section 2 with the shape parameterization technique, utilizing a set of constraints and objective function to select an optimal design. Section 5 shows the result from the global response assessment of the selected optimal designs in extreme sea-states DLC 1.6, as highlighted in IEC 614003–2 2019 and in Leimeister et al. (2020b). Section 6 summarizes the conclusions and future recommendations from this study.

#### 2. Methodology

The optimal geometric design perturbation of a model with parameterization technique, within an MDAO framework, to change the shape geometry of a FOWT spar substructure and the evaluation of the new dynamic response characteristics, requires an iterative process which can be expensive computationally, with regards to time and cost. As detailed in Section 1, the primary goal of this work is to explore innovative design of the spar's geometric shape, and integrate this design concept into a state-of-the-art MDAO framework to search, and identify an optimal design from a rich design space. This establishes a detailed geometric shape parameterization method for FOWT substructures and enables a comprehensive search of the design space using an optimization algorithm.

The methodology approach details a high-level review of the state-of-the-art design analysis and optimization technique in Section 2.1. A detailed description of the process framework and tools for design and optimization is highlighted in Section 2.2.

The glue code integrating the MDAO framework (exploration and exploitation phase and the constraint verification phase) is highlighted in Fig. 1.

#### 2.1. State-of-the-art in design, analysis, and optimization

# 2.1.1. Parameterization techniques for FOWT support structures

Most of the parameterization techniques used in designing FOWT platforms mainly alters the radii, draft, length or breadth of the platform as discussed in Wayman (2006). This approach mainly serves to increase or reduce the whole platform or a section of the platform – and can be classified as holistic scaling or sectional scaling. Holistic and sectional scaling has the capability of effectively increasing or reducing the volumetric dimension of the structure while the use of parametric curves can also alter the shape of the design for effective design space exploration.

Wayman (2006) made significant early advancements in creating cutting-edge, economically viable floating platforms designed to support 5 MW wind turbines in water depths ranging from 30 to 300 m. Wayman (2006) developed a frequency-domain analysis tool to conduct a integrated structural, aerodynamic, and hydrodynamic analysis of the FOWT system. This work was progressed by Tracy (2007) in a study presenting a full multidiscipline integrated dynamic analysis of FOWTs, which allows for a variable design investigation of both the turbine concepts and mooring systems. Their findings demonstrate that the Pareto optimal structures for a full multidiscipline integrated dynamic analysis of the wind turbine, the floater, and the mooring system, taking into account wind and wave loading conditions, are a barge platform ballasted with concrete or a narrow deep drafted spar. The parameterization done in Tracy (2007) only varies the draft and the diameter of the floater; hence, limiting the design space that can be explored.

To further enrich the design space, there is need for effective control of the design variable not just from global shape control but local control of the shapes of the structure. To achieve this objective, Birk (2006) introduced the polynomial spline parametric modelling technique. Birk

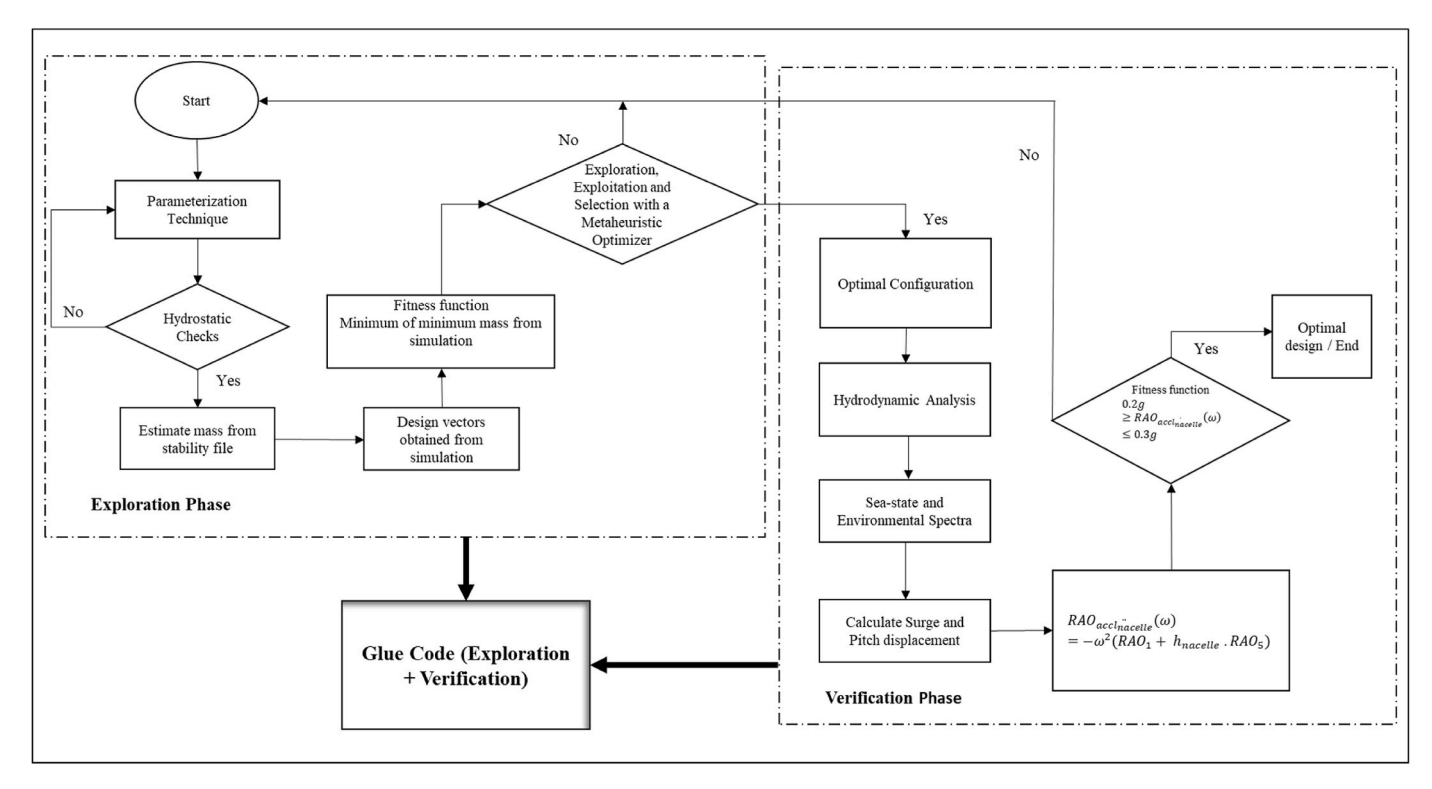


Fig. 1. Flowchart of framework methodology – (Exploration and Verification Phases).

(2006) was able to present an optimization system/framework which integrates spline parametric modelling tools, numerical modelling tools – potential flow theory and controlled with optimization algorithm with specified objectives and constraints that enables the system to design offshore platforms with enhanced offshore operating qualities. The local shape control approach is explored in this study.

## 2.1.2. Design analysis and optimization tools

Geometric shape optimization is an important component of engineering design. For example, in the offshore industry, the essential component of an optimal shape design process is the structural geometry modeler, an appropriate mesh creator, discipline AHSE solvers and a state-of-the-art optimizer. Some of the cutting-edge work conducted in FOWT design and optimization sector are discussed in this section.

2.1.2.1. Parametric modelling technique. As highlighted in section 1, a detailed cutting-edge review of geometric parametric modelling of a system has been provided in Samareh (2001). For this framework, the parametric modelling technique of use is the polynomial spline (NURBS option).

NURBS are polynomial curves with the capability and flexibility to create a large spectrum of shapes from points to splines, lines (implicit and explicit) and conic sections. NURBS are particularly useful for 3-D modelling as they make it simple for designers to perturb control points. Both control points and weights define NURBS, and it also requires minimal data for its definition. NURBS surfaces have many good properties amongst which are visual fairness and perfect smoothness in comparison to design surfaces represented by discrete meshes. Unlike other parametric curves like B-Spline and Bezier curves, NURBS can accurately depict a lot of the parametric implicit curves (Farin, 1990; Samareh, 2001). A representation of a NURBS is shown in Eq. (1).

$$\overline{R}_{(U)} = \frac{\sum_{i=1}^{n} \overline{P}_{i} W_{i} N_{i,p}(\nu)}{\sum_{i=1}^{n} W_{i} N_{i,p}(\nu)}$$

$$(1)$$

Where  $\overline{P}_i$  represents the control points,  $W_i$  depicts the weights and  $N_{i,p}(\nu)$  represents the ith B-spline basis function of p-degree. non-uniformity allows some segments of a specified shape (in between points) to be shortened or extended in relation to other segments in the global shape. Rationality allows the capability to assign varying importance to different points in a shape, based on their positional relationships to other objects.

For the purpose of this study, the NURBS curve was utilized from the commercial software DNV SESAM Genie. Sesam Genie has a cubic B-Spline library with both curvature (C2) and slope (C1) continuities which can be converted to NURBS with control point shape modification capability of the panel and finite element mesh creation for frequency domain assessment.

2.1.2.2. Discipline solvers and optimizers. The solvers used for the disciplinary analyses are either in frequency domain or time domain.

2.1.2.2.1. Frequency domain. The frequency domain approach, while less accurate in comparison to the time domain approach, has been widely adopted in the oil and gas sector. It facilitates the evaluation of the response spectrum of the system based on the wave spectrum of the site and the response amplitude operator (RAO) of the system (Journée and Massie, 2000; Patel, 2013). The resultant system of equation of motion that governs the frequency domain method in regular wave is highlighted in Newman (2018). In depth details of frequency domain approach and its application on offshore platforms for FOWT system are presented in Newman (2018) and reviewed in Ojo et al. (2022a). The frequency domain approach is implemented in commercial software like WAMIT and HydroD/WADAM – used in this study.

2.1.2.2.2. Time domain approach. The time domain method employs a coupled dynamic model in the time domain, allowing for the consideration of nonlinear forces and transient conditions. To get a more accurate assessment of these values, statistical analysis can be used to find the important statistical parameters for responses like displacements, velocities, and acceleration. Comprehensive details of the time domain approach is presented in Journée and Massie (2000) and reviewed in Ojo

#### et al. (2022a).

For the FOWT system, Jonkman (2007) led the development a sector-wide accepted tool for analysing the discipline coupled dynamic response assessment of a HAWT. This tool facilitated coupled dynamic analysis of a FOWT coupled with floaters, adhering to the IEC 61400-3 guidelines. It is now incorporated into OpenFAST, one of the most widely utilized medium-fidelity simulation assessment tools for FOWTs. In the present work, OpenFAST is used for verification of the proposed design's dynamic response.

## 2.1.3. Optimizers

The formulation of an optimization problem is determined by its objectives (concave or convex). The definition of a general design optimization problem involves minimizing or maximizing an objective function while adhering to specified design constraints. The representation of this statement for a single objective function problem is shown in Eq. (2).

$$egin{align*} \min_{x \in \mathbb{R}} J(x) \ subject to egin{cases} xlower \leq x \leq xupper \ h_i(x) = 0; i = 1 \ to \ m \ g_j(x) \leq 0; j = 1 \ to \ p \end{cases}$$

Where x is a k-dimensional vector of design variables with defined lower and upper bounds, J(x) represents a single objective function, m denotes the number of equality constraints and p denotes the number of inequality constraints.

Optimization algorithms or computational methods to find the best solution or optimal value of a given problem within a defined set of constraints are divided into two categories: Gradient-Based (GB) optimization algorithms and Gradient-Free (GF) optimization algorithms.

GB techniques are iterative techniques that utilise the gradient or derivative information of the cost function during each iteration (Yang, 2019). These methods are particularly effective for finding local minima in high-dimensional, non-linearly constrained convex problems. Examples of the GB algorithms are the Broyden-Fletcher-Goldfarb-Shanno (BFGS), Newton Powell, Feasible Sequential Quadratic Programming, and the Sequential Least Square Quadratic Programming method.

GF algorithms are typically characterised by their superior search efficiency and robustness. This contrasts with GB algorithms, which often struggle with local minima in optimization problems involving multimodal objective functions (Hegseth et al., 2020). Examples of the GF algorithms are: Genetic Algorithm, Pattern Search Optimization Algorithm, Particle Swamp Optimization Algorithm, Nelder Mead and Simulated Annealing.

As a result of the superior search efficiency that characterizes the GF optimizers, a substantial amount of FOWT substructure optimization work coming up are adopting the GF approach. Some examples of these novelle approach can be seen in Hall et al. (2013) where a FOWT hull and mooring optimization study is conducted across the oil and gas sector's traditional platform concepts (spar, semi-submersible and TLP) using the genetic algorithm (GA). Application of the GA to single and multi-objective optimization in this study shows the selection of unconventional designs that highlights the need for objective refinement.

Karimi et al. (2017) enhanced this work by using the Kriging-Bat optimization algorithm to define the exploration and exploitation of the design space. This approach resulted in a. better correlation between cost and substructure design in comparison to the findings of Hall et al.

Other works on optimization related to a FOWT system for GB and GF optimizers with a multidisciplinary feasible framework are reviewed in the Ojo et al. (2022a).

#### 2.2. Framework development and tools

The MDAO framework derived for discipline integration as shown in Fig. 1 is to enable the effective design, analysis, and optimization of multiple disciplines within the framework while resolving the optimization task. The optimization problem in this study is to minimize the cost function which is the reduction in steel material mass required for the platform's design. The multidisciplinary design and analysis (MDA) with the structural discipline design and shape parameterization technique, the platform's hydrostatic analysis and the frequency domain hydrodynamic assessment is conducted to predict the system's response with the panel method widely used in solving potential flow problems as shown in Fig. 1.

The optimization process within the framework in Fig. 1 is used for selecting the feasible hydrostatic design variants that satisfies the constraints specified within optimization algorithm. The selection of the optimal design is driven by pattern search optimization algorithm (Torczon and Trosset, 1998). Verification of the most optimal feasible design variant is assessed within the framework where all the FOWT disciplines – aerodynamics, hydrodynamics, servo dynamics and electrodynamics (AHSE) are coupled together in medium fidelity time domain assessment (OpenFAST) to verify the constraints specified are within the allowable design limits.

The tools utilized include the Python suite, MATLAB for optimization, and DNV's Sesam Genie with a NURBS library that features control point perturbation and shape alteration of panel geometric models and finite element mesh production of custom-shaped spar design variants. The modified finite element mesh representing the selected platform design is imported into HydroD/Wadam to analyse the system's responses in the frequency domain.

#### 2.2.1. DNV suite

Three main DNV tools used within the MDAO framework are Sesam GeniE, HydroD and Wadam highlighted herein:

2.2.1.1. Sesam GeniE. Sesam GeniE is a software for advanced geometry modelling of engineering shapes - beams, plates and shells (DNV, 2021). It is also used for load modelling amongst which includes equipment load, wind and wave loads and gravitational loads of floating structures. This study has made use of the free-form parametric curves in Sesam GeniE to effect a change in the shape of the platform for optimization purposes within the framework.

2.2.1.2. DNV HydroD. The HydroD suite is used for hydrostatic assessment for stability and equilibrium of the floating structure (DNV, 2021). It offers analysis workflows for running Wadam, allowing the computation of multiple floating equilibrium positions based on mass and compartment filling fractions which is estimated using the glue or interface code detailed in section 2.2.1.

2.2.1.3. WADAM. Wadam is a hydrodynamic assessment tool for estimating wave-structure interaction for fixed and floating structures in a marine environment (DNV, 2021). Wadam performs hydrodynamic analysis in frequency domain using airy waves and its development is built on the potential theory (radiation/diffraction) approach for structures with large volume (DNV, 2021; DNVGL Høvik, 2019).

2.2.1.4. OpenFAST. OpenFAST is a multi-physics, multi-fidelity tool for simulating the coupled dynamic response of wind turbines (OpenFAST, 2023). OpenFAST is an open-source tool that integrates aerodynamics, hydrodynamics, elastodynamics and servodynamics engineering models for wind turbines in time domain. It is used to verify the frequency domain limit state results are still acceptable in the non-linear time domain assessment conducted this study.

#### 2.2.2. Glue/interface code

This study developed a glue code to integrate the disciplines and operations within the framework as highlighted in Fig. 1. The main programming languages used in the glue code are Python and MATLAB. The glue code facilitates the dynamic transfer of the random design variable within the specified bounds of the optimizers to the NURBS control points within the panel modelling tool Sesam GeniE. This panel modelling process is the platform for a successful exploration of the design space for further characterization with design objective and constraints that leads to the selection of optimal designs.

In addition to passing design variables from optimization algorithm to the control points along the NURBS curve for panel shape modelling, other tasks within the glue code are highlighted herein:

- Estimate the ballast filling fraction
- Pass design variables for Compartment shape from the optimization algorithm
- Assess optimization constraints in the hydrostatic leg
- Assess optimization objective function
- Sets framework to run automatically.

#### 2.2.3. Exploration phase

The first phase is the exploration stage, which is focused on the hydrostatic analyses to select the designs that satisfies the stability requirements and also assess the objective function of design with the minimal mass. The optimization problem is defined in the exploratory phase as detailed in Section 2.2.2.1. For this work, the optimization problem is a non-convex, non-Linear objective with a set of non-linear constraints as defined in Equation (2) and detailed in Section 2.2.2.1. In the exploration stage, a multidisciplinary design analysis and optimization scheme using curve parameterization to change the shape of the floater design is conducted. The polynomial spline used for the design is the cubic polynomial ordered NURBS curve from the commercial software DNV SESAM Genie. The design vector is composed by the control points altering the radii at different points across the draft of the spar, as shown in Table 5 of Section 3.1. The parameterized NURBS curve is autonomously converted to a panel model and FEM files to prepare the designed structure for hydrostatic and hydrodynamic analyses. Three FEM files are generated from the cubic polynomial NURBS curve for hydrostatic and hydrodynamic assessment - panel model, compartment model and the total mass model.

2.2.3.1. Definition of the optimization problem. This work uses the local propagation properties of the NURBS curve with a PSM optimization algorithm to solve a defined optimization problem. The optimization problem in Equation (2) has a non-linear and non-convex objective with a series of non-linear constraints. To resolve this optimization problem, a number of methodologies can be investigated as detailed in Kochenderfer and Wheeler (2019). A series of no free-lunch theorems by Wolpert and Macready (1997) indicates that it is not feasible to determine the best optimizer for a specific problem beforehand and the only way to identify the most effective approach is to empirically test multiple algorithms and evaluate their performance. Nonetheless, PSM has been used in this work (Findler et al., 1987; MathWorks, 2021), supported by findings in other disciplines as detailed in Saenz-Aguirre et al. (2022); Torczon and Trosset (1998).

Moreover, based on floating foundation optimization conducted in Frank Lemmer et al (2016) considering simple algorithm (GA, Particle swarm algorithm and PSM approaches), pattern search was recommended as the preferred optimization solver integrated with the dynamic simulations to explore and exploit the design space.

Since the starting point influences the convergence of all the PSM algorithm, a multi-start strategy is employed for this study (Laguna and Martí, 2003). The starting points for the optimization process have used 50 random points equally spread within the design domain defined by

the non-linear constraints of the optimization objective in Equation (2). The optimization approach is executed using the Matlab 2017 environment.

The optimization problem in this study is defined with the goal of minimizing the objective function as highlighted in Equation (2). The objective function  $-\mathbf{J}$  to be minimized in this optimization problem is dependent on the design variables x and the inequality constraints -g. The parameters that make up the optimization problem to generate a novel shaped optimized platform are detailed in Sections 2.2.2.1.1 to 2.2.2.1.3.

 $2.2.3.1.1.\ Design\ variables$ . The design variable for modelling the spar is a set of 14 control points along the NURBS curve and a draft value of 120 m for each static pitch design considered. The control points are located in steps of 10 m apart from the tower base to the platform's keel. Mathematical expression and description of the variables is presented in Table 1.

An example of the optimal design variables for design use cases assessed is shown in Table 7. The design space is defined by setting the design variables within bounds – lower and upper bounds. The lower bound is the minimum value that can be passed into the control points to vary the substructure's shape locally and the upper bound is the maximum value to be passed into the control points. The lower and upper bound values set for the shape optimization assessment in this chapter is  $1 \, \text{m}$  and  $7 \, \text{m}$  respectively.

2.2.3.1.2. Objective function. The objective function for minimization is the structural mass of the geometrically modified spar, and the output is dependent on the hydrostatics assessment of the design models. The structural mass has the capability of directly influencing the material cost, labour cost (manufacturing), transportation cost and cost of installation (increase or decrease in the size of lifting equipment). General expression for minimizing objective function is highlighted in Equation (2). The mathematical expression for calculating the mass of the optimized substructure which id the main objective in this work is shown in Equation (3).

**Table 1**Definition of design variables.

Platform design variables	Description	Compartment design variables	Description
<i>x</i> <sub>1</sub>	Radius at tower base	-	-
$x_2$	Radius at MSL	$x_1$	Radius at MSL
$x_3$	Radius at 4 m	$x_2$	Radius at 4 m
	below MSL		below MSL
$x_4$	Radius at 12 m	$x_3$	Radius at 12 m
	below MSL		below MSL
<b>x</b> <sub>5</sub>	Radius at 30 m	$x_4$	Radius at 30 m
	below MSL		below MSL
$x_6$	Radius at 40 m	$x_5$	Radius at 40 m
	below MSL		below MSL
<i>x</i> <sub>7</sub>	Radius at 50 m	$x_6$	Radius at 50 m
	below MSL		below MSL
$x_8$	Radius at 60 m	$x_7$	Radius at 60 m
	below MSL		below MSL
<b>X</b> 9	Radius at 70 m	<i>x</i> <sub>8</sub>	Radius at 70 m
	below MSL		below MSL
$x_{10}$	Radius at 80 m	$x_9$	Radius at 80 m
	below MSL		below MSL
$x_{11}$	Radius at 90 m	$x_{10}$	Radius at 90 m
	below MSL		below MSL
$x_{12}$	Radius at 100 m	$x_{11}$	Radius at 100 m
	below MSL		below MSL
$x_{13}$	Radius at 110 m	$x_{12}$	Radius at 110 m
	below MSL		below MSL
$x_{14}$	Radius at 120 m	$x_{13}$	Radius at 120 m
	below MSL		below MSL

$$mass = \rho_{steel} *Vol_{Substructure}$$

$$Vol_{Substructure} = \int_{-draft}^{10} A_x(x) dx$$
(3)

Where  $\rho_{steel}$  represents the steel density,  $Vol_{Substructure}$  represents the substructure's volume,  $A_x$  represents the sectional area and (x) represents the sectional height along the length of the substructure. For the optimization framework utilized in this study, a multi start approach is employed to eliminate local minima issues; hence, the minimum of the minima is selected as the optimal design variable in the explored design space.

2.2.3.1.3. Optimization constraints. With a focus on shape parameterization within the optimization framework in this research work and to simplify amount of design variables, the draft length is kept constant and constrained to a value of 120 m and the set of design variables radii that are input into the control points are randomly varied in every iteration.

The main constraint driving the platform's shape alteration and optimization inside the framework is the static pitch inclination constraint derived from the restoring and inclining equation of the FOWT system with a thrust force of 785 KN at the nacelle to estimate the inclining moment. Derivation of the static pitch angle is detailed in Equation (4) (Collu and Borg, 2016) and represented schematically in

Fig. 2

$$\frac{F_T(z_{hub} - z_{MLA})}{\left(\rho_w g I_y + F_b z_{CB} - F_w z_{CG} + C_{55,moor}\right)} \le \theta_{max} \tag{4}$$

where  $F_T$  represents the thrust force induced by the wind speed,  $z_{hub}$  represents the turbine's hub height and  $z_{MLA}$  is the center of mooring line assembly,  $\rho_w$  is the density of water, g is the gravitational acceleration,  $I_y$  is the second moment of waterplane area X axis,  $F_b$  is the force of buoyancy,  $z_{CB}$  represents the center of buoyancy,  $F_w$  is the system's weight,  $z_{CG}$  is the system's center of gravitational acceleration,  $C_{55,moor}$  is the mooring stiffness, and  $\theta$  is the static pitch angle of inclination/tilt. The expression  $\rho_w g I_y + F_b z_{CB} - F_w z_{CG} + C_{55,moor}$  in Equation (4) represents the minimum total stiffness leading to the maximum angle of inclination.

The static pitch angle derived should not exceed the allowable maximum operational static pitch inclination set for the FOWT system. This non-linear constraint is key in estimating the optimized platform's masses and three use cases of 5 deg, 7 deg and 10 deg static pitch angles are considered. Other constraints developed along with the static pitch angle constraint are the floatability constraint, imposed as having a ballast mass greater than zero, and the nacelle acceleration constraint. Summary of these constraints are shown in Table 2.

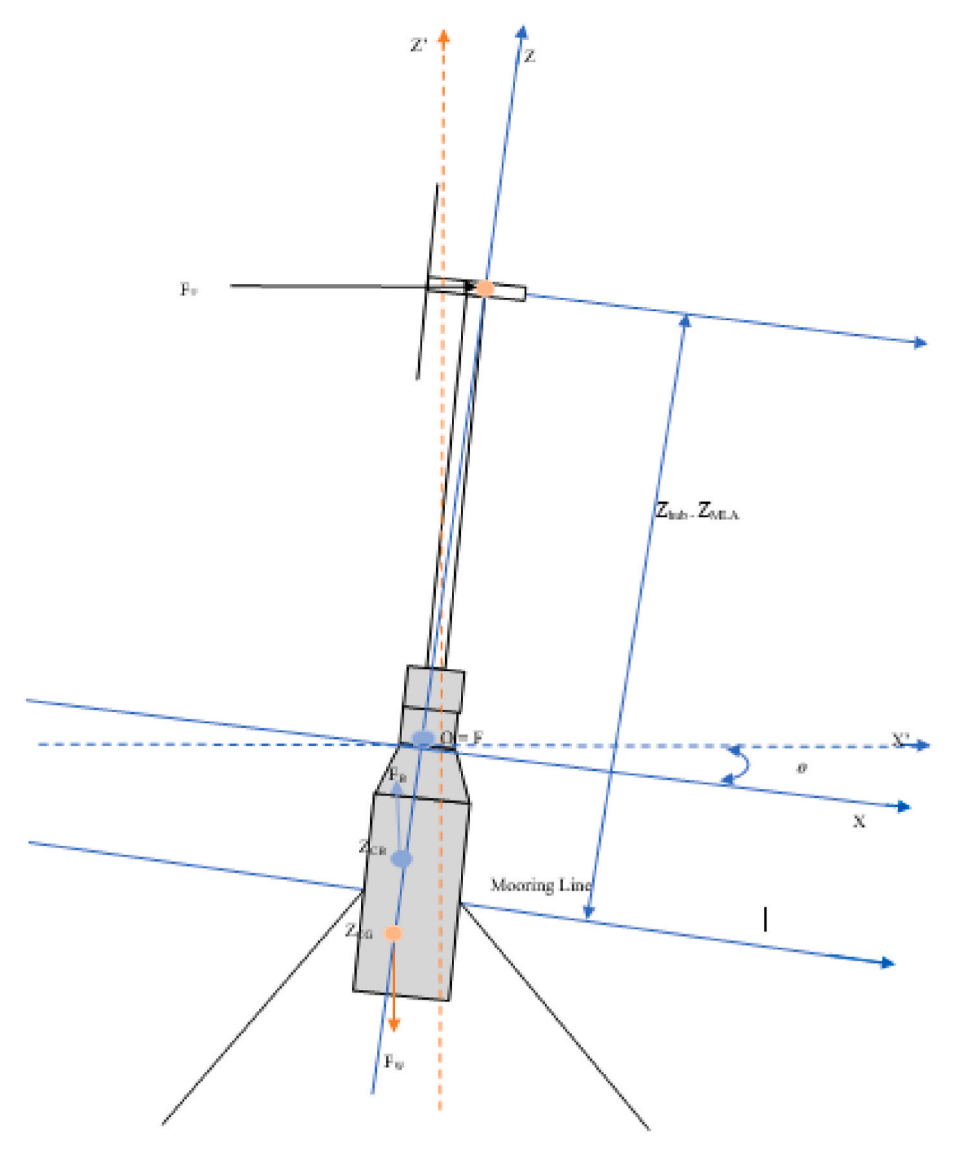


Fig. 2. Reference points and forces of a typical spar FOWT.

Table 2
Optimization constraints.

Inequality Constraint	Formal expression	Description
g <sub>SP_05</sub>	$g_{SP=05} \leq 5^{\circ}$	Maximum static pitch below 5 deg
8 <sub>SP_07</sub>	$5^{\circ} \leq g_{SP-07} \leq 7^{\circ}$	Maximum static pitch greater than
		5deg and less than of equal to 7 deg
8SP_10	$7^{\circ} \le g_{SP\_10} \le 10^{\circ}$	Maximum static pitch greater than
		7deg and less than of equal to 10 deg
<b>g</b> ballast	$ extit{g}_{ballast} \in \mathbb{R}$	Calculated ballast a positive real
		number
nacelle <sub>acceleration</sub>	$nacelle_{acceleration} \leq 2.943$	Nacelle acceleration less than 30 % of gravitational acceleration.

The physical rationale to the constraints are detailed below:

- The nacelle acceleration is selected according to DNV standard of less than 0.3 g to eliminate excessive motion in the nacelle to prevent it from damage or crack from excessive oscillatory motion of components within the nacelle assembly.
- Static pitch angles are imperative to prevent excessive motion of the FOWT system from environmental loading, avoid damage from these motions and improve energy yield capture from the wind.
- A positive ballast is essential to ensure the hydrostatic stability of the FOWT design i.e., the total weight of the FOWT system equates to its buoyancy. The FOWT's hydrostatic stability is a fundamental requirement prior to assessing the system's response to hydrodynamic loading.

2.2.3.2. Design exploration. The optimization definition explores the design space based on the dimension of the design variable to be explored. Three components of the substructure design to be modelled for each optimization iteration are the panel model, the compartment model and the total mass model as detailed in section 2.2.2.2.1 to section 2.2.2.2.3.

2.2.3.2.1. Panel model. This is the model defining the wet geometry of the platform below the sea water level. A couple of assumptions made in the panel model are highlighted in Journée and Massie (2000) amongst which includes inertia loads is the dominant loads, fluid is incompressible, irrotational and inviscid. To ensure a standard panel model, a CAD model providing a detailed geometric representation of the platform within the fluid domain is conducted with Sesam Genie. This includes information about its shape, size mass and dimension. The next step is to apply a mesh density size to the platform and a triangular mesh with 0.7 m size was applied to the CAD model. A load case is created, and a dummy hydrostatic pressure is applied to the platform's draft below the MSL to create the wet geometry required for the velocity potential formulation and FEM generation. The generation of a finite element mesh to discretize the fluid domain. This involves dividing the continuous geometry from the CAD model into a finite number of smaller interconnected nodes and elements. This finite element mesh generated provides the numerical representation of the substructure beneath the MSL used in the hydrostatic phase.

2.2.3.2.2. Compartment model. This is carefully designed taking into consideration the fact that the shape of the compartment must change as the panel shape or outer shell changes, since different design vectors are passed through the iteration process. A code was developed which was integrated with the JavaScript code in Sesam Genie to align the compartment shape with the shape of the outer shell of the platform and also calculate the equivalent ballast mass or compartment content filling fraction to stabilize the platform in the hydrostatic analysis phase.

The filling fraction is estimated from the hydrostatic result file. This is done adjusting the overall mass of the system to the equivalent displaced mass of the platform. The ratio required to work the filling fraction for the ballast mass withing the compartment model is highlighted in Equation (5).

$$Fill Fraction = \frac{Pfm_{dispmass} - Pfm_{mass}}{System_{totalmass} - Pfm_{mass}}$$
 (5)

where  $Pfm_{dispmass}$  is the displaced mass of seawater by the platform.

 $Pfm_{mass}$  is the steel mass or corresponding platform's material mass;  $System_{totalmass}$  is the system's total mass – sum masses of platform, mooring, tower and rotor nacelle assembly.

2.2.3.2.3. Total mass. The overall mass model of the system, including the rotor nacelle assembly, the tower, the platform panel, and the compartment are modelled to account for the system's total, which is used for estimating the restoring moment of the FOWT system. This is also essential for estimating the structural mass moment of inertia in all degrees of motion for the FOWT system. To accurately model the total mass; the nacelle's mass and center of gravity, the substructure mass and center of gravity, and the tower mass and its center of gravity and are accounted for in a unique name set or model subset. A finite element mesh is generated for this named set to capture the geometric and physical properties and serve as a numerical representation of the structure in the hydrostatic phase.

The analysis part of the MDAO framework assesses the hydrostatics and hydrodynamics characteristics of the system, using the potential theory approach, and it is discussed in detail and verified for the reference OC3 FOWT system, modelled with the NURBS curvein section 3.1, with the response of the hydrodynamic coefficient added mass, damping, force excitation and the values of the response amplitude operators showing a good alignment with the published data.

Coupling the optimization algorithm with the design and analysis stages completes the autonomous MDAO framework. The MDAO framework is automated with a set of MATLAB and Python codes to ensure that the whole MDAO cycle, from the definition of the design vector to the hydrostatic and hydrodynamic analyses, to the evaluation of the cost function and the definition of the next design variable, is fully autonomous, i.e., no manual input is required. The iterative process is continuous until the design space has been substantially explored and exploited. The control points' alteration as a result of the autonomous input of the design vectors by the pattern search method (PSM) along the length of the NURBS curve is schematically illustrated in Fig. 3. The straight lines used in Fig. 3 can be described as a parametric curve of zero continuity - hence, the sharp edges as the radii of the control points changes. The NURBS curve utilized within this study has C<sup>2</sup> (slope and curvature) continuity, which ensures continuous smoothness of the NURBS curve at the control points along the spar. Details of the integrated parametric design within the MDAO framework, to select feasible design that satisfies the stability requirements, are discussed in Section 4.1 to 4.3.

#### 2.2.4. Verification phase

Verification stage is focused on the hydrodynamics of the selected designs from the exploration phase, analysed with low-fidelity frequency domain hydrodynamic analysis tools - Sesam HydroD (WADAM/WAMIT) - and verification of the results with a medium-fidelity hydrodynamic tool - OpenFAST. The process required for this verification stage is as detailed in the flowchart within Fig. 1. This verification phase is more of confirmation of the constraints within the MDAO framework are still within the allowable values from the design codes and standards in a time domain assessment when non-linear forces and considered.

A standalone case study for an OC3 platform with a normal sea-state is analysed hydrodynamically to evaluate the system's response and verify the assessed responses with a medium fidelity time domain tool as detailed in section 3. Similarly, a detailed hydrodynamic analysis with a severe seastate using DNV1.6a design code and standard with the selected optimized shape variants from the design space is detailed in section 5 with results highlighted in section 5.4.1. The verification of the design with medium fidelity time domain analytical tool is presented in

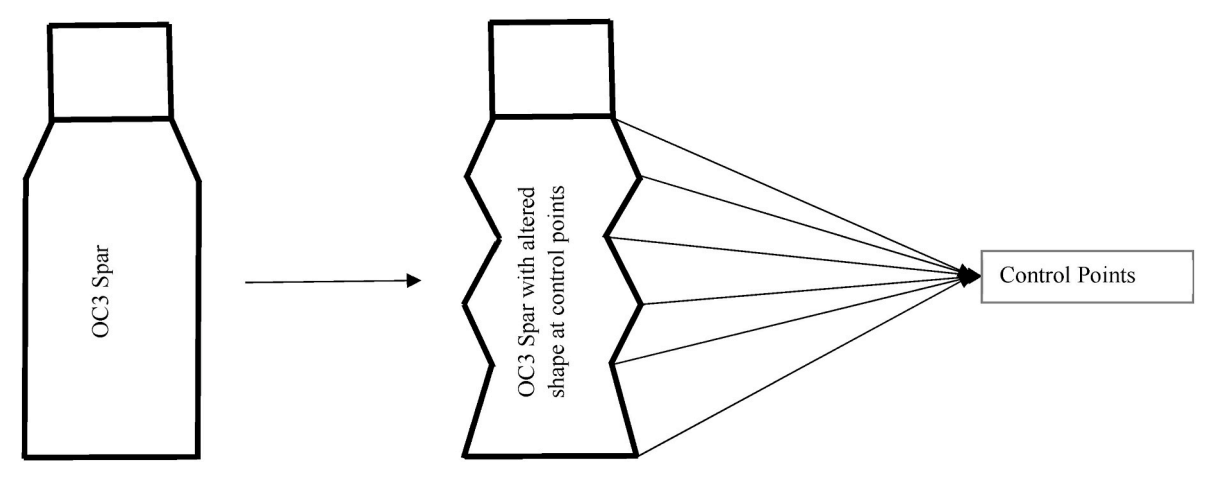


Fig. 3. Variation of control points along the parametric curve (Ojo et al., 2022b).

section 5.4.2.

#### 3. OC3 substructure - 5 MW spar-buoy case study

The OC3 spar-buoy floater is an axis-symmetric ballast stabilised platform coupled to a wind turbine and moored with three steel catenary mooring lines. The fairlead ate connected at a depth of 70 m below SWL with a radius of 5.2 m from the centreline of the platform. The anchors are located in 320 m water depth and a radius of 853.87 m from the platform's centreline. It is a derivative of the Hywind spar (Siemens, 2009) and it is modified for the NREL 5 MW reference wind turbine (Jonkman et al., 2009). Comparison of the structural parameter values shows that, in addition to improved and reduced draft of the actual systems, the dimensions fall in between those of the Hywind Demo for a 2.3 MW wind turbine and the Hywind Scotland floater supporting a 6.0 MW wind turbine (Leimeister et al., 2020a).

An OC3 spar-buoy sketch is shown in Fig. 4 with the floater model highlighted in Fig. 5. The geometric variables for the spar are shown in Table 3. The structural parameters amongst which include the mass of the spar including ballast, center of mass, moments of inertia and additional linear damping in surge, sway, and yaw are detailed in Jonkman (2010), and highlighted in Table 3. The hydrostatic force of buoyancy from the displaced water by the spar is 80708100 N (Jonkman, 2010). To match the Hywind floater's characteristics, an additional linear damping of 100000 Ns/m is applied in the surge and sway degree of freedom while additional linear damping of 130000 Ns/m and 13000000Nms/rad in heave and yaw degrees of freedom respectively as detailed in Jonkman (2010).

The 5 MW NREL reference turbine is installed on the OC3 Spar to complete the FOWT system. A detailed description of the platform geometric properties, platform structural properties, tower and hub properties, and structural properties of the wind turbine topsides are presented in detail in Jonkman (2010), and highlighted in Tables 3 and 4 respectively.

#### 3.1. Frequency domain - potential flow theory OC3 spar

The modelling process of a FOWT system or FOWT substructure can be done with a host of state-of-the-art design tools based on various simulation codes with different modelling capabilities for handling AHSE calculations as detailed in (Cordle and Jonkman, 2011). Some of the tools highlighted in Cordle and Jonkman (2011) are Open-FAST/FAST, Bladed, SIMO/RIFLEX (Simulation of Marine Operations) etc. Most of these design tools are time domain analysis tools; hence, more computationally expensive.

For this work, t the tools used for the design and hydrodynamic assessment of the OC3 spar are from the Sesam suite, specifically GeniE  $\,$ 

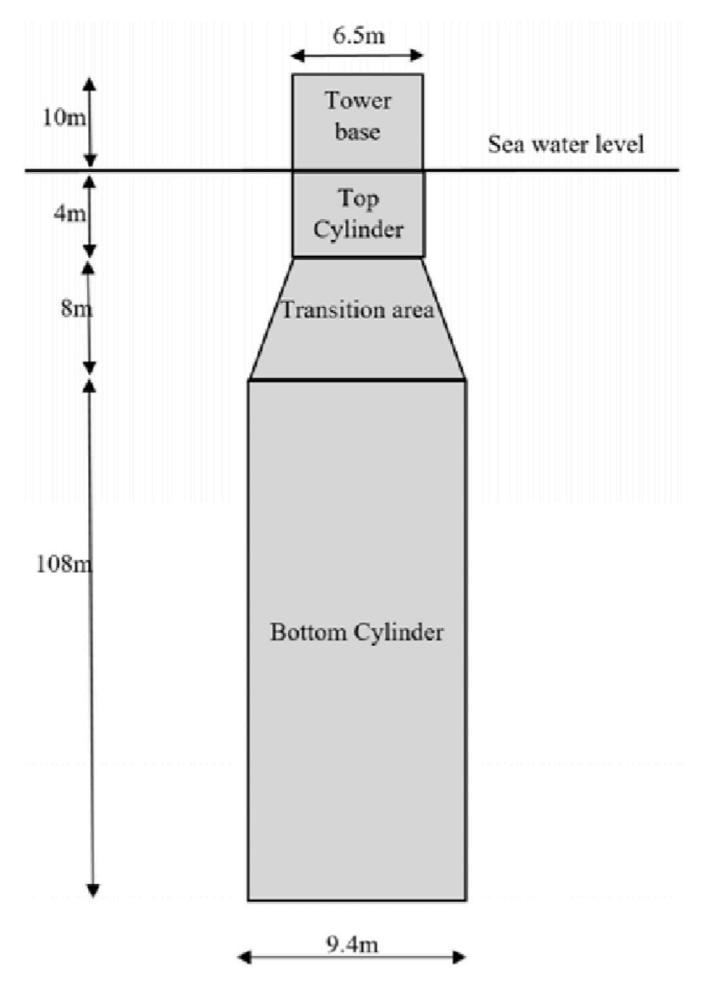


Fig. 4. OC3 spar Sketch.

and Wadam. GeniE is an effective software for conceptual or detailed design of engineering structures – plates, beams, and shells. It features a detailed library of geometric tools that facilitate the creation of lines, splines (cubic splines, B-splines, and NURBS) and surfaces for modelling engineering structures. The NURBS curve is utilized for the panel model of the OC3 spar-BUOY with 14 control points (13 below sea water level and 1 above) depicting the radii along the length of the spar-buoy. Each green grid in Fig. 5 represents the control point in which the NURBS curve passes and a table of these control points is shown in Table 5. The



Fig. 5. NURBS model of an OC3 Spar FOWT in Sesam GeniE.

Table 3
OC3 spar geometric variables and structural properties (Jonkman, 2010).

Parameters	Dimensions (m)
Top circular diameter	6.5
Top cylindrical height	4.0
Connecting piece top diameter	6.5
Connecting piece base diameter	9.4
Length of connecting piece	8.0
keel to sea water line (Draft)	120.0
Base circular diameter	9.4
Base height	108.0
Mass of platform plus ballast	7,466,330 kg
Pitch inertia of platform	4,229,230,000 kgm <sup>2</sup>
Platform's center of mass	89.92 m
Yaw inertia of platform	164,230,000 kgm <sup>2</sup>

 $\begin{tabular}{ll} \textbf{Table 4} \\ \textbf{Tower and hub dimension and structural properties for OC3 floating system.} \end{tabular}$ 

Parameter	Values per Literature
Tower top elevation	87.6 m
Tower base elevation	10.0 m
Hub height - (m)	90.0 m
Diameter at tower top	3.87 m
Wall thickness at tower top	0.019 m
Diameter at tower base	6.5 m
Wall thickness at tower base	0.027 m
RNA mass	350000 kg
Tower mass	249700 kg
Tower's center of mass	43.4 m

platform's thickness is estimated by numerical iteration to match the buoyancy mass. This estimate is based on the mass ratio of steel to buoyancy of 0.13 for a spar platform (Anaya-Lara et al., 2018; Bachynski and Collu, 2019). Based on the steel mass to buoyancy mass ratio, the iterative process estimates the value of thickness that corresponds to the desired value of the system's total mass to be equivalent to the buoyancy mass. After several iterations, a watt thickness value of 0.04 m along the length of the spar correspond to the buoyancy mass/total mass of the system. The tower and RNA are represented in GeniE with a dummy beam, and the calculated center of mass of the tower and RNA is assigned to the dummy beam. The OC3 spar-buoy is integrated with the dummy beam and the coupled system is meshed in GeniE suite. Three FEM files are required from the modelling stage. The first is the FEM file for the panel model for potential flow theory i.e., the wetted surface, the second FEM mesh required is for the compartment model, and the third FEM file represents the total structure i.e., the platform and the dummy load representing the tower and the RNA.

The FEM files are transferred to Wadam for hydrodynamic evaluation of the response of the system. Using the NURBS parametric technique to design the OC3 spar platform with data from Table 5 in Sesam GeniE and performing hydrodynamic analysis with the potential flow theory discussed in Section 2.1 with the WADAM option in the Sesam HydroD tool, a set of simulated results verified with literature results from Jonkman (2010) are highlighted in this section. The compared result highlighted is the translational surge, heave and rotational pitch displacement RAOs with a wave heading of zero degrees as shown in Fig. 6.

The findings in Fig. 6 verifies the fidelity of using the potential flow approach and conducting simulation in computationally less expensive low-fidelity frequency domain tool with the alignment of the results of the simulation model with results from literature.

# 3.2. Time domain coupling and response verification (medium fidelity tools)

An adequate time domain analytical assessment is conducted with OpenFAST - a medium fidelity tool with the capability of using the Cummings equation time domain analysis approach highlighted in Section 2.1, taking into consideration the non-linear forces acting on the system.

The potential flow model from Wadam generates frequency dependent added mass, radiation damping, and it also produces first order wave forces. The frequency-dependence added mass and radiation damping are included in the time domain Cummins equation.

In assessing the time domain with OpenFAST, the substructure files (added mass and radiation damping file, first order wave excitation force/moment file, and the hydrostatic file) from the frequency domain analysis, discussed in Section 3.1, are used by OpenFAST, and a time

**Table 5**OC3 Spar NURBS curve control points below sea water level.

OC3 Radii along vertical axis representing B-spline	Height (m)	0	4	12	30	40	50	60	70	80	90	100	110	120
	Radius (m)	3.25	3.25	4.7	4.7	4.7	4.7	4.7	4.7	4.7	4.7	4.7	4.7	4.7

**Table 6**Motion response statistics (OC3 model vs NURBS model).

Degree of Freedom	Maximum OC3	Maximum NURBS Coupled	Maximum Percentage Error	Mean OC3	Mean NURBS Coupled	Mean Percentage Error	Minimum OC3	Minimum NURBS Coupled	Minimum Percentage Error
Surge	26.22 m	26.02 m	0.77	22.73 m	23.51 m	3.32	18.47 m	20.79 m	11.16
Sway	-0.25  m	−0.27 m	7.41	-0.34  m	-0.33  m	3.03	-0.44  m	−0.39 m	12.82
Heave	0.09 m	−0.35 m	125.71	-0.49  m	-0.53  m	7.55	−0.94 m	−0.68 m	38.24
Roll	$0.32^{\circ}$	$0.29^{\circ}$	10.34	$0.24^{\circ}$	$0.25^{\circ}$	4.00	$0.17^{\circ}$	$0.20^{\circ}$	15.00
Pitch	5.91°	5.58°	5.91	4.60°	4.85°	5.15	$2.52^{\circ}$	3.59°	29.81
Yaw	0.65°	$0.40^{\circ}$	62.50	$0.10^{\circ}$	$0.10^{\circ}$	0.00	$-0.48^{\circ}$	$-0.20^{\circ}$	140.00

**Table 7** Optimal models design data.

Case A	Height (m)	0.0	4.0	12.0	20.0	30.0	40.0	50.0	60.0	70.0	80.0	90.0	100.0	110.0	120.0
	Radius (m)	4.11	4.36	3.85	6.13	6.67	2.46	3.73	5.68	2.65	4.51	5.56	5.72	3.58	3.56
Case B	Height (m)	0.0	4.0	12.0	20.0	30.0	40.0	50.0	60.0	70.0	80.0	90.0	100.0	110.0	120.0
	Radius (m)	1.00	6.74	4.12	4.36	1.93	5.95	4.01	6.69	3.01	2.72	5.31	5.20	4.91	4.01
Case C	Height (m)	0.0	4.0	12.0	20.0	30.0	40.0	50.0	60.0	70.0	80.0	90.0	100.0	110.0	120.0
	Radius (m)	1.91	2.34	3.00	6.29	5.70	3.25	5.49	6.14	1.64	4.30	4.91	2.85	6.78	1.25

Table 8
Seastate and environmental data Leimeister et al. (2020b).

Wave and Wind Parameters								
H <sub>s</sub> (m)	10.37	Spectrum's significant wave height						
T <sub>p</sub> (sec)	14.70	Spectrum's peak period						
Peak/Gamma factor	3.30	Peak shape parameter						
$\sigma_1$	0.07	Spectral width parameter $\leq$ peak angular frequency						
$\sigma_2$	0.09	Spectral width parameter > peak angular frequency						
$U_{ref}$ (m/s)	12	Rated wind speed						

domain simulation is conducted considering a sample design load case corresponding to a normal environmental sea state of 6 m significant wave height, and 10s peak period and a rated wind speed of 11.4 m/s. The motion response statistics for the comparison between the two models with the aforementioned sea state is presented in Fig. 7.

# 4. Shape design parameterization, analysis and optimization of OC3 variant models

This section details the use of polynomial curves and its integration with a state-of-the-art optimizer to effectively explore the design space and select optimal design variants, with varying shapes satisfying the stability design requirements for offshore floaters. The optimal variants selected will be subject to further analysis to verify their suitability.

## 4.1. Geometric shape design and variants generation

The NURBS curve is used to design the panel of the spar platform with 14 control points and 13 segments as highlighted in Table 3. The NURBS curve is a generalization of B-Spline; hence, it has important geometric properties of B-Spline (Samareh, 2001) amongst which are:

- The order or degree chosen for the curve is independent of the control points.
- Unlike a Bezier curve, NURBS/B-Spline have the local propagation property which enables effective control of the local shape around the control points of interest.
- NURBS/B-Splines are invariant under Affine transformation. This
  ensures the curve doesn't change under transformations like translation, rotation, scaling and shearing

#### • It has a convex hull property and a partition of unity property

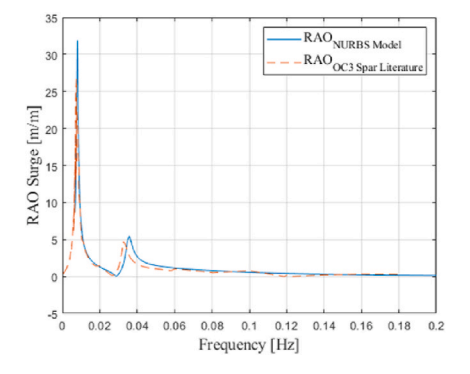
The local propagation property of the NURBS curve is very essential for the geometric shape variation and optimization that will be extracted from the axis-symmetric spar floater. The varying parameter along the fixed length of the spar is the radii at all the specified control points. The variation of the radii along the length of the spar is automated and it follows an iterative process where the set of radii from the specified objective function is written into the modelling file in Genie before a hydrostatic analysis is conducted in HydroD.

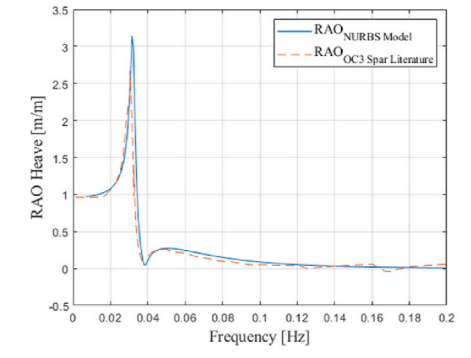
#### 4.2. Integration with optimization algorithm

The optimizer utilized in this parametric shape alteration work is the meta-heuristic pattern search optimization algorithm method (PSM). PSM is among the most frequently used methods designed to resolve gradient free optimization problems.

The use of an optimization algorithm like Pattern Search is of an advantage with its global convergence capability as it doesn't get stuck in local minimum (Palacio-Morales et al., 2021). For this work, a multi-start method is encoded within the pattern search algorithm. The multi-start enhanced Pattern Search algorithm strategically samples the solution space of the optimization problem. This technique alternates between two phases for a predetermined number of global iterations. The first stage develops a solution, while the second stage aims to enhance the result. The algorithm final output is the best overall solution, which is the best of the local minima within the global design space. On completion of the sampling process, the global optimum is selected from the list of local minima as the solution that mostly satisfies the objective function. To produce an effective approach of producing high-quality solutions, the interaction between the two phases balances search diversification with search improvement. A multi-start approach enhance global search and exploration capability, eliminates the dependence on single initial condition, and minimises the risk of converging to suboptimal solution.

The nature of the optimization problem is described in Eqn. (2) of section 2.1 in which the solution is to minimize the objective function (mass of the substructure).





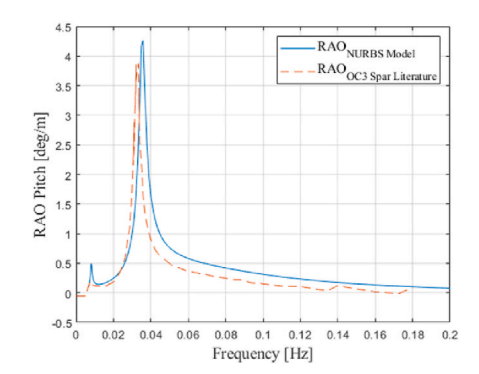


Fig. 6. RAOs in Surge, Heave and Pitch (NURBS data vs literature data).

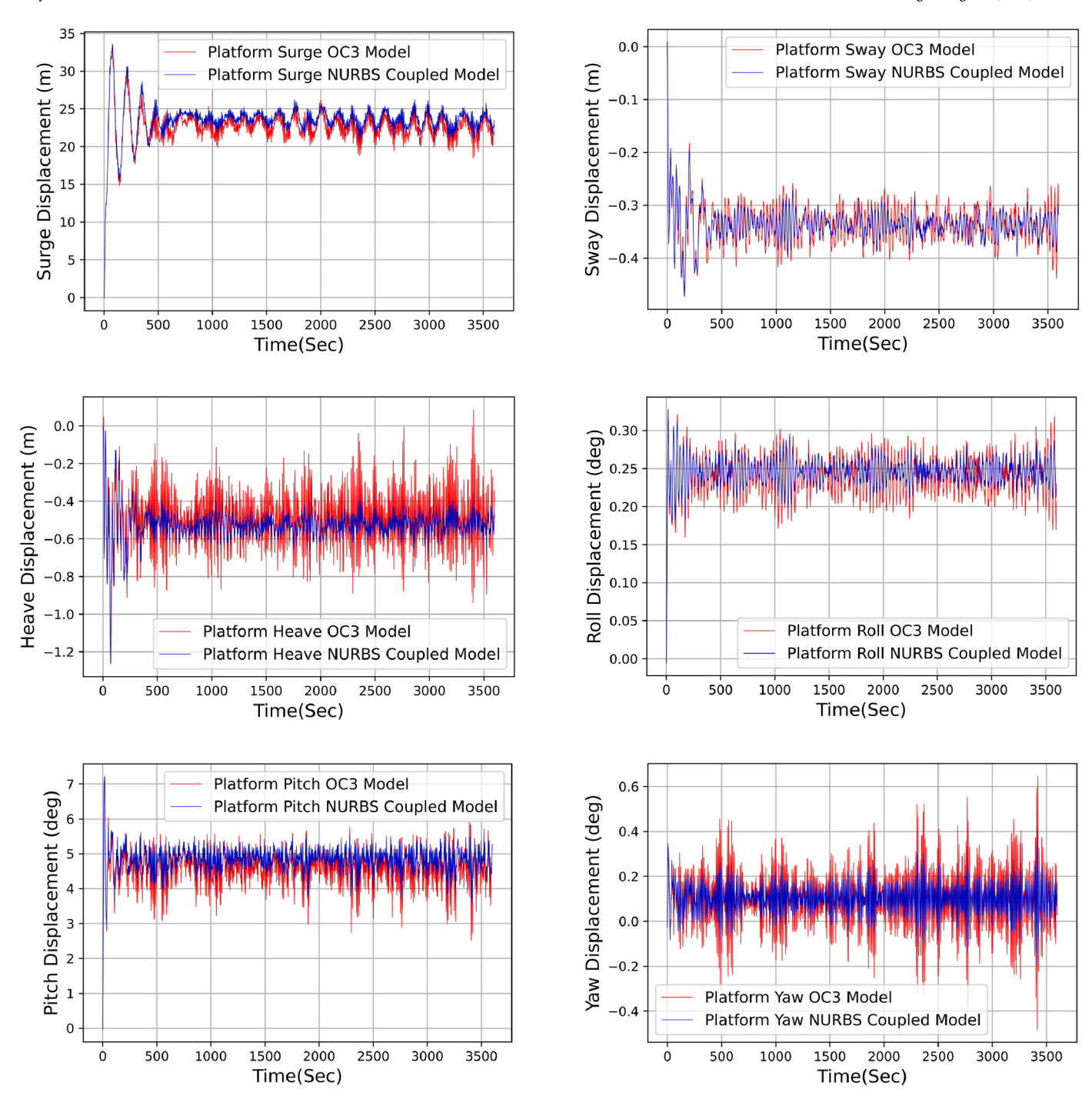


Fig. 7. NURBS Platform Coupled Platform Response vs NREL 5 MW OpenFAST Design Response.

# 4.3. Objective function and constraints

This optimization study focuses on a single objective function: minimizing the cost of the steel material used for the spar platform, which is directly related to the mass of steel. The ballast cost is assumed to be negligible. The study considers four constraints listed below:

- 1. The nacelle acceleration must remain within the allowable acceleration limit (<0.3~g)
- 2. Ballast mass must be greater than zero to ensure floatability
- Positive pitch initial stiffness is required to prevent unfeasible solutions.

 The static pitch angle must not exceed the maximum allowable operational static pitch angle

The maximum static pitch angle of tilt is defined across three cases:  $5^{\circ}$ ,  $7^{\circ}$ , and  $10^{\circ}$ , in the context of the hydrostatic analysis phase highlighted within process in Fig. 1. Based on the defined constraints and objective function, the MDAO framework is executed following the steps highlighted below:

 A sampling size "n" is defined within the multi-start code embedded in the PSM. "n" is an integer and for the purpose of this frame work, "n" is set as 50.

- 2. Bounds of upper and lower limits for the design vector variables are set within the PSM (to write the design variables into the NURBS curve within DNV Sesam Genie' Java Script (JS) file). The upper bound and lower bound diameter values of 7 m and 1 m respectively are specified within the PSM.
- 3. Three finite element mesh (FEM) models are generated from running Sesam Genie. The first FEM is the Panel FEM model for potential flow analysis in HydroD. The second FEM is the compartment FEM model for ballasting the spar for structure stability. The third FEM model represents the entire structure i.e., the substructure (platform) and the superstructure (tower and rotor nacelle assembly) represented with a point mass.
- 4. The three FEM files are hydrostatically assessed in HydroD for each iteration.
- 5. The results are benchmarked against the static pitch angle constraint, and a pool of feasible results are created from the samples
- 6. The results are assessed with the sole objective of minimizing the mass of the structure and the most feasible/optimal design is selected for each of the static pitch angle constraints of  $5^{\circ}$ ,  $7^{\circ}$  and  $10^{\circ}$  respectively.
- The selected/most feasible design is hydrodynamically assessed in frequency domain and in a medium-fidelity time domain tool (OpenFAST).

#### 4.4. Selection of optimal design variants

The control points and corresponding radii along the vertical axis for the three optimal designs selected are presented in Fig. 8 and Table 7, and labelled cases A, B and C, corresponding to maximum pitch angles of  $5^{\circ}$ ,  $7^{\circ}$ , and  $10^{\circ}$  respectively. Each case is interfaced with the NREL 5 MW wind turbine rotor nacelle assembly.

The selected control points in Fig. 8 and Table 7 are the outputs carefully evaluated from the MDAO framework of this study. The platform for the MDAO framework is detailed in section 2.2.1 where design variables are randomly passed from the design variable boundaries specified in the GF pattern search optimization algorithm into the NURBS curve to model the platform's wet geometry panel in Sesam Genie. The next step within the iterative loop is detailed in section 4.3. This MDAO framework loops through thousands of iterations and a set of feasible designs are selected. However, in this study, the design variables (radii along the control points) that mostly satisfied the specified objective function of global minimum mass against each static pitch angle constraint of  $5^{\circ}$ ,  $7^{\circ}$  and  $10^{\circ}$  are selected as cases A, B and C respectively.

This study is a proof of concept that uses free-form curve (NURBS) within an MDAO framework specifying a set of constraints and a single objective function of minimizing mass to reduce the quantity/mass of material (Steel) required for manufacturing with the possibility of lowering the capital cost of the FOWT platform. However, achieving this objective of capital cost minimization from reducing material for manufacturing the platform can be jeopardized by the additional costs incurred from manufacturing complex shapes. The limitation is highlighted in section 1.3 and potential solution also highlighted in section 6.

# 5. Global response assessment of optimal design variants and results

#### 5.1. Global limit state assessments of the design variants

The global limit states assessment considered for this study are the pitch angle, nacelle acceleration and translational motion under severe sea state as stipulated in IEC-61400-3-2 (2019).

#### 5.1.1. FOWT pitch angle

The system's pitch angle is an essential design and optimization constraints used in exploiting and selecting the optimal design from a large design space. As highlighted in Section 4.4, the pitch angle constraints specified in the design and optimization framework are  $5^\circ, 7^\circ$  and  $10^\circ$  respectively. A conventional value of  $10^\circ$  is used based on Kolios et al. (2015) and Leimeister et al. (2020b). For the purpose of this study, global response assessment is conducted for the  $5^\circ, 7^\circ$  and  $10^\circ$  pitch angles of the FOWT system.

#### 5.1.2. Nacelle acceleration

The nacelle consists of sensitive components amongst which are the gearbox, generator, and bearings, essential for electricity production. As highlighted in Rasekhi Nejad et al. (2017), a typical limit for maximum allowable nacelle acceleration is set at 30 % or less of acceleration due to gravity, which translates to values less than 2.943 m/s<sup>2</sup>.

#### 5.1.3. Translational motions

As a result of the wave and wind loading on a FOWT system, the system will drift during operation. However, the drift varies between different FOWT system configurations based on the station keeping system adopted i.e., the translation motions in a TLP FOWT system is highly restricted as a result of the tensions in the moorings employed for station keeping as highlighted in Bachynski and Moan (2012). For other FOWT design configurations like the spar, there are no publicly

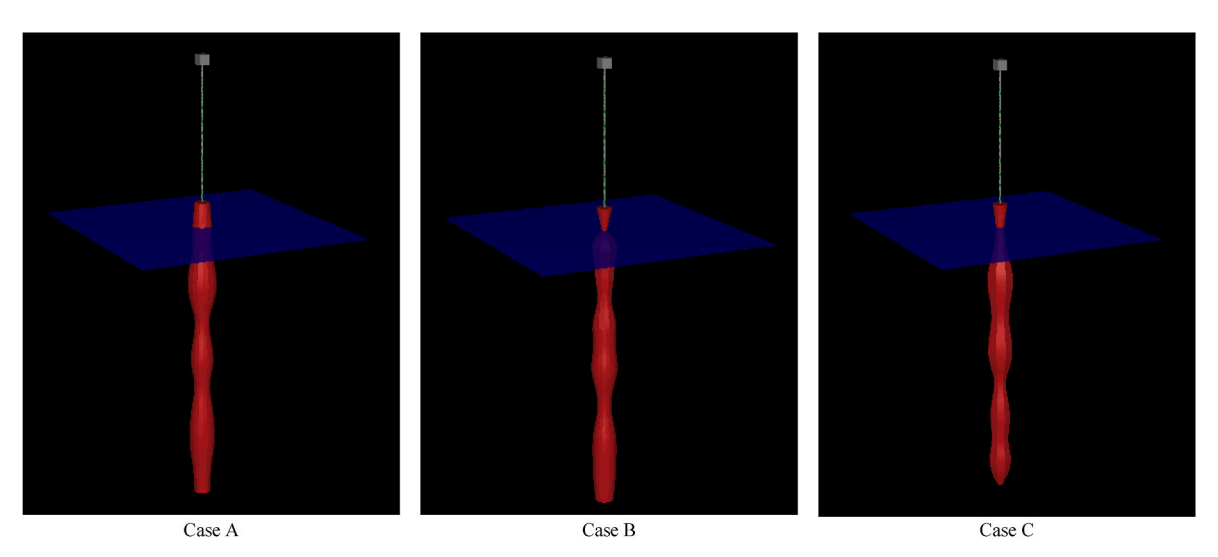


Fig. 8. Optimal design models from pattern search optimization algorithm method.

available limits for the translational motion as the power cable's permissible motion is the critical criteria in limiting the translational motion of the FOWT system (Leimeister et al., 2020b). The total translational displacement (combined surge, sway, and heave motion) has two parts that must be distinguished in analysing translational motion: the static displacement, which is primarily caused by the aerodynamic thrust acting on the wind turbine rotor, and the dynamic displacement, which represents the oscillatory motion caused by wind and wave loading. In Leimeister et al. (2020b), the dynamic displacement is constrained to a max value of 20 % of water depth, while Kolja Müller et al (2017) the maximum excursion/offset of the floater in surge, which includes both the static and dynamic components, is less than 50 % of the water depth. This study will consider translational motion value of 15 % water depth for more conservative results i.e., 15 % of the water depth (48 m of translational displacement) is a much-constrained allowable design requirement than 50 % water depth (160 m of translational displacement).

#### 5.2. Design load case

The global response assessment of the optimal design cases highlighted will be conducted using the conservative DLC1.6a highlighted in International Electrotechnical Commission standard (IEC) - IEC61400-3-1 (2019) and IEC-61400-3-2 (2019). DLC 1.6a is a very conservative load case matrix with the following characteristics:

- The DLC 1.6a uses normal current and turbulent wind models while considering a severe irregular sea state. The FOWT system is generating power in a normal production mode.
- This DLC 1.6a highlights key criteria for a wind turbine in an area where waves are dominant. The severe irregular sea state leads to considerable fluctuations in wave elevation time series, resulting in the excitation of the FOWT system in oscillatory motion.
- DLC 1.6a is expected to produce critical values for the nacelle acceleration as the dynamic translational motion if the FOWT system is wave sensitive.

The DLC1.6a is selected for this study to carefully access the response of the FOWT system's motions in all degrees of freedom and also the nacelle acceleration in a severe seastate for conservative design and analysis of the system.

# 5.3. Environmental parameters

The wind and wave environmental parameters considered for this study are highlighted in this section.

#### 5.3.1. Wind

The 5 MW spar FOWT system is operated at the rated wind speed of 11.4 m/s. The rated wind speed is used in this study for conservative purpose as the system is expected to experience the largest response at the rated wind speed. This ensures the most onerous response of the FOWT system is captured. For the purpose of time domain assessment in this study, a Kaimal wind spectrum is utilized to the turbulence wind inflow in this study and like in Jonkman (2007) the turbulence intensity category B with a power law shear exponent of 0.14 is used for normal turbulence model. The DLC 1.6a is for power production in severe seastate condition for normal operation event. The simulation is repeated six times utilizing six different seeds, and therefore generating six different set of wind velocity time signals having the same average wind speed, turbulence spectrum, and turbulence intensity.

#### 5.3.2. Wave

For DLC1.6a, severe sea state is utilized for the global response assessment of the FOWT system. The wave spectrum considered in this assessment is the JONSWAP wave spectrum. The site's sea-state is from

Leimeister et al. (2020b) and taken for an assumed water depth of 320 m.

The JONSWAP wave spectrum expression is detailed in DNVGL Oslo (2018) highlighting the required spectral parameters for estimating the wave spectrum for a defined sea-state.

Fig. 9 shows the calculated wave power spectrum from the detailed JONSWAP expression in DNVGL Oslo (2018) over a duration of 4 s–198 s with an interval of 1 s. A step of 1 s is used as HydroD/WADAM cannot accommodate more than 200 vectoral frequencies. The peak frequency of the power spectrum is shown at circa 0.068 Hz, which is corresponding to the peak period of 14.7 s. The estimated maximum power for the wave spectrum is about 305 m $^2$ /Hz.

#### 5.4. Results and discussion

The results and discussion are grouped under the frequency domain and time domain analytical approach.

#### 5.4.1. Frequency domain global dynamic response analysis

This section highlights the system's response based on the environmental conditions for modelling the JONSWAP wave spectrum. The frequency domain panel model utilized in the MDAO framework in Section 4 for selecting the optimal design based on stability analysis is used in conducting the hydrodynamic assessment. This method gives a high-level estimate of the system's responses in different degrees of freedom. The responses are assessed for the three cases (A, B and C or 5 deg, 7 deg and 10 deg static pitch angles respectively) compared to the baseline OC3 5 MW FOWT system. Fig. 10 details the surge, heave, and pitch RAOs and horizontal nacelle displacement motion across the three design cases considered along with the OC3 spar. It is shown in Fig. 10 that the peak response frequencies in surge, heave, pitch and nacelle displacement motions are around the low frequency region. With first order wave loads usually occurring between 0.04 Hz and 0.2 Hz, the peak responses highlighted in Fig. 10 are around the lower threshold of the first order wave or beyond the peak frequency range of the first order wave load. Also, the nacelle horizontal displacement RAO represents the sum of the surge RAO and the product of the pitch RAO and the FOWT system's hub height. The increase in magnitude of the peak nacelle horizontal displacement RAO in comparison to the surge and pitch RAO is shown in Fig. 10.

An important feature in the result from the hydrostatic mass of the optimal cases (A, B and C) based on static pitch inclination constraints of 5 deg, 7 deg and 10 deg and the OC3 model with the NURBS curve is that

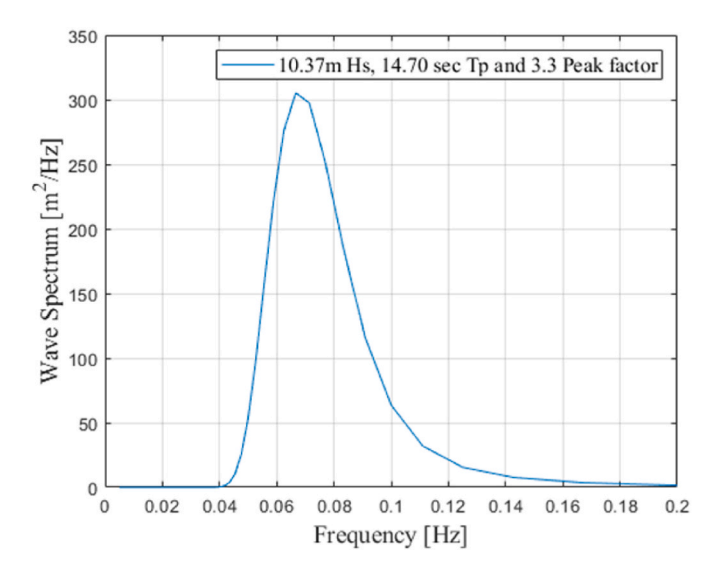


**Fig. 9.** Wave Spectrum- 14.7s peak period and 10.37 m significant wave height.

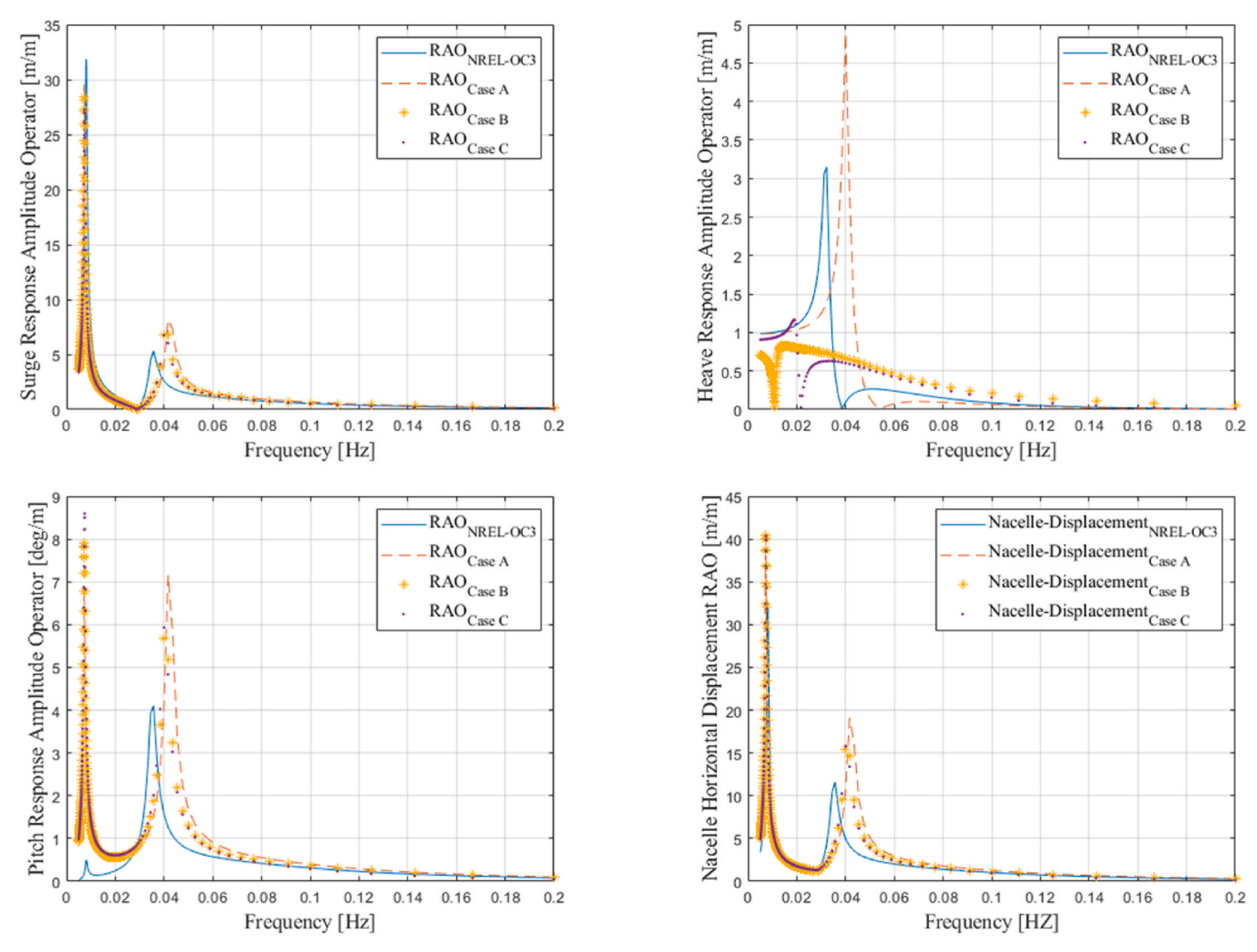


Fig. 10. RAO in Surge, Heave, Pitch and Nacelle displacement for optimal cases and baseline OC3 spar.

the OC3 model has the largest mass. However, it is shown from the other results that as the static pitch angle constraints increases from 5 deg, 7 deg and 10 deg, the mass of the optimal/feasible design selected from the optimization framework is reduced as seen in Table 9. Estimated cost of the platform is highlighted in Table 9 using the cost of steel per tonne of 537GBP from Ioannou et al. (2020).

For this optimization framework in which the objective function is lowering the steel mass of the structure, an effective way of achieving the objective function is increasing the pitch angle constraints. For conservatism, the maximum pitch angle constraint for this study is set at  $10^{\circ}.$ 

Fig. 10 shows that of all the three optimal variants selected, case A design variant exhibits the highest peak motion responses in surge, heave, pitch, and nacelle horizontal displacement, with values of approximately 30 m/m, 4.9 m/m, 7 deg/m, and 40 m/m, respectively. This analysis excludes viscous forces; thus, lower peak values are anticipated when viscous forces are considered.

Table 9
Platform steel mass and cost.

Platform	Steel mass (Tonnes)	Steel cost (GBP)
OC3	1763.53	947.02 E+03
Case A	1750.03	939.77 E+03
Case B	1708.43	917.43 E+03
Case C	1641.17	881.31 E+03

The system's dynamic response in the 6DOFs, for each of the cases assessed, are different from the reference system's dynamic response due to a few factors that affect the natural frequency and the damping. These factors include:

- the mass distribution of the platform COG and mass matrix;
- the added mass matrix frequency dependent;
- the hydrostatic and mooring stiffness matrices,
- $\bullet$  and the radiation damping frequency dependent.

All these factors are dependent on the wet geometry of the floating substructure, and in turn determine the RAOs of the platform – and, in particular, the largest effects can be observed in the heave DOF, as highlighted in Fig. 10.

To develop a fundamental understanding of how the aforementioned factors change the RAOs, a simplified decoupled, 1-DOF analysis, based on prime principles, is provided.

Given the mass (M), the heave added mass at the infinite frequency ( $A_{33}$ ), the hydrostatic ( $C_{hyd,33}$ ) and mooring ( $C_{moor,33}$ ) stiffness in the heave DOF, as derived through the numerical analyses conducted (Table 10), the 1-DOF, uncoupled heave (undampened) natural frequency can be derived with Equation (6).

$$F_{n,33(undampened)} = \sqrt{\frac{C_{hyd,33} + C_{moor,33}}{M + A_{33}}}$$
 (6)

**Table 10**Heave natural frequency estimate from mass added mass and stiffness.

	OC3 Benchmark	Case A	Case B	Case C
Mass (Kg)	8.16 E+06	8.13	7.67	7.34
		E+06	E+06	E+06
Heave Added mass	2.26 E+02	3.27	5.80	3.67
		E+02	E+02	E+02
Heave Hydrostatic Stiffness	3.43 E+05	5.43	4.21	1.25
(N/m)		E+05	E+04	E+05
Heave Mooring Stiffness	1.19 E+04	1.19	1.19	1.19
(N/m)		E+04	E+04	E+04
Damping at Natural Frequency (NS/m)	1.32E-01	6.91E-01	2.98E-03	5.44E-01
Heave Wave Load (N/m)	82891	166743	15077	29881
Heave Frequency (Hz)	0.0322	0.0400	0.0122	0.0180

From the results in Table 10, the 5 deg configuration (CaseA) presents a higher heave natural frequency in comparison with the benchmark (OC3 model) configuration. Taking Equation (6) into consideration, coupled with the scenario of a constant heave mooring stiffness across both configurations with slight difference in the total mass, the higher natural frequency in Case A in comparison to the baseline model can explained as highlighted below.

Although, the added mass for Case A is circa 45 % larger than the added mass for the baseline model. The circa 58 % higher hydrostatic stiffness more than compensate for the added mass increase; hence, pushing the heave displacement response of Case A at its natural frequency to circa 29 % higher than the Benchmark OC3 model's heave displacement response at its natural frequency. However, for Case B and Case C, while the added masses are circa 156 % and 62 % respectively greater than the corresponding added mass for the benchmark model, the hydrostatic stiffnesses of Case B and Case C are respectively 88 % and 64 % lower than the corresponding hydrostatic stiffness of the benchmark OC3 model. This occurrence reduces the heave natural frequency of Case B and Case C with regards to the benchmark model's heave natural frequency by 58 % and 33 % respectively.

Furthermore, an estimate of the magnitude for the peak heave responses at the natural frequencies of all the cases is conducted with the heave wave load at the natural frequencies are highlighted in Table 10. This assessment is conducted using the response amplitude operation expression in Equation (7) (Journée and Massie, 2000) utilizing the mass of the structure, Mooring and hydrostatic stiffness in heave and the heave added mass and heave radiation damping highlighted in Table 10. The calculated result presented in Table 11 shows a good alignment with the corresponding simulated results shown in Table 11. Although the calculated and simulated results show good agreement, there are still slight differences between the two results. This difference is due to the simplification of the calculated results i.e., using the hydrodynamic parameters - radiation damping, stiffness, mass, and added mass in only 1DOF. However, for the simulated results, there are contributions from coupled motions in other degrees of freedom. Furthermore, additional linear damping from Jonkman (2010) is added on top of the hydrodynamic load in the three translational DOF and the vaw rotational DOF in order to align the free-decay responses as highlighted in Jonkman

$$RAO_{j} = \left| \sum_{k=1}^{6} \frac{X_{k}}{-\omega^{2} (M_{kj} + a_{kj}) + i\omega b_{kj} + c_{kj}} \right|$$
 (7)

**Table 11**Estimate of Heave displacement response magnitude at natural frequency.

	OC3 Benchmark	5DEG	7DEG	10DEG
Simulated Heave Response (m/m)	3.17	4.70	1.21	1.01
Calculated Heave response (m/m)	3.31	4.03	1.68	0.70

Fig. 11 shows the response spectrum for nacelle horizontal displacement with the corresponding dynamic response (RAOs) and the wave spectrum for all the three optimal design variants and the OC3 spar FOWT system.

Considering the specific sea state from Table 8 and the dynamic response in all DOFs for all the cases (A-C and OC3 spar) in Fig. 11, the range of frequencies over which the nacelle's response amplitude operators is significant does not substantially mirror or overlap the frequency ranges with which there is a substantial wave energy. The nacelle RAO is well decoupled from the wave spectrum analysed; hence, it ensures that the area below the system's response spectrum which is proportional to the energy in the waves absorbed by the platform in the surge and pitch degrees of freedom contributing to the nacelle displacement is relatively small. This is a characteristic of a well-designed platform.

The estimated nacelle accelerations RMS values for the OC3 model and the 3 variants are shown in Table 12 and they are all below the  $1.962\,\mathrm{m/s^2}$  or 20 % of acceleration due to gravity value recommended as the benchmark for nacelle acceleration used in this study as highlighted in Section 5.1.2.

An observation from the frequency domain study is that for cases A, B and C, their dynamic response is higher than the OC3 design's dynamic response. However, the variant cases A, B and C responses still satisfy the allowable design constraints from standards used in assessing the optimal designs. This shows the OC3 design is much more conservative than the optimal variant cases A, B and C. This conclusion is only valid for this study as only one design load case for severe seastate is being considered (DLC 1.6a). This observation might not be valid if other design load cases and other constraints like environmental impact assessment and structural are imposed; hence, this can be explored in future work.

#### 5.4.2. Time domain analysis

The simulation of the coupled FOWT system in time domain allows the system's response evaluation to wind and wave loads including nonlinear forces, which cannot be represented in frequency domain approach. For this work, the frequency domain analytical approach (Potential Flow theory) detailed in Section 2 is verified against the results obtained with OpenFAST. OpenFAST is a wind turbine simulation tool capable of a detailed time domain coupled AHSE analysis of an offshore/onshore wind turbine system (OpenFAST, 2023). To represent the optimal geometric shaped platform selected in section 4 with OpenFAST, the hydrodyn and elastodyn source code has not been changed. However, the hydrodyn and elastodyn input files are updated to account for the hydrodynamic and structural changes in the optimal design variant cases A, B and C. As highlighted in Jonkman (2007), the hydrodyn module accounts for the following:

- Linear hydrostatic restoring stiffness of the floating system;
- Contributions of added mass and damping from linear wave radiation, accounting for free-surface memory effects;
- Incident wave excitation from linear diffraction in both regular and irregular sea states;
- Nonlinear viscous drag induced by platform motion and incident wave kinematics.

For the coupling process, the hydrostatic restoring stiffness is obtained from the WAMIT output files in the frequency domain analysis conducted in Section 4. The added mass and damping contributions and the incident wave excitation from linear diffraction are carefully extracted from the HydroD output on completion of the frequency domain analysis in WADAM. Finally, the displaced volume of water when the platform is in its stable position obtained from the stability analysis in frequency domain is set in the hydrodyn module to represent the optimal design variant assessed. The elastodyn module's file is updated with the optimal platform's mass, the center of mass' distance

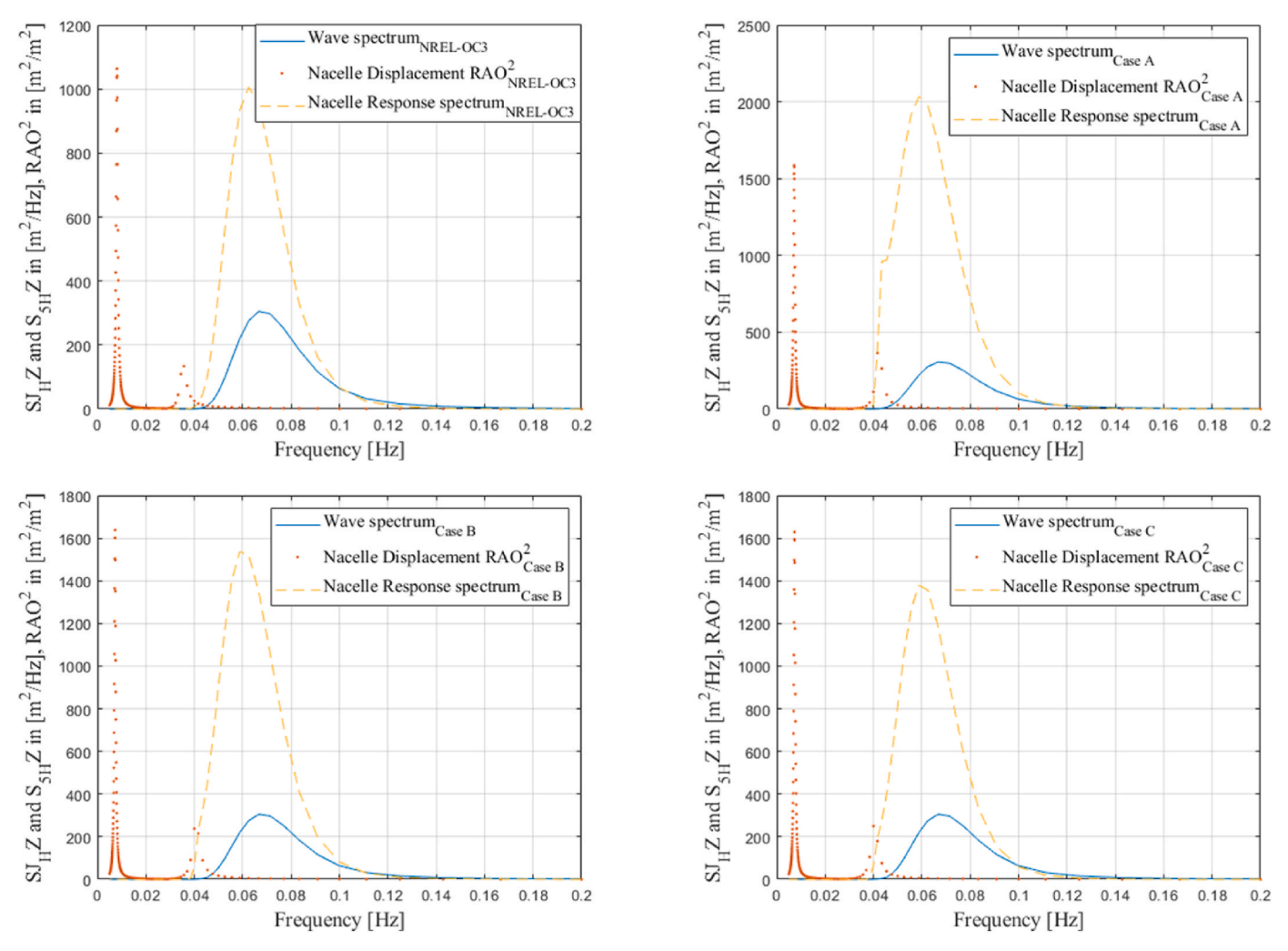


Fig. 11. FOWT system's Nacelle horizontal displacement response spectrum for optimal cases and baseline OC3 spar.

**Table 12**Nacelle acceleration RMS – frequency domain.

	OC3 baseline	Case A	Case B	Case C
Zeroth Moment	0.0060	0.0117	0.0089	0.0075
Nacelle RMS	0.0777	0.1083	0.0942	0.0868

to the mean sea level, the calculated platform's rotational inertia in the roll, pitch and yaw DOFs. The updated elastodyn and hydrodyn modules are simulated with the aerodyne and servodyn module to have a holistic multidisciplinary simulation of the interfacing disciplines within a FOWT system.

The two analyses conducted for the coupled FOWT system from the optimal geometric platform selected in Section 4 are:

- Free decay test
- FOWT system's dynamic response analysis

5.4.2.1. Free decay analysis. The free decay analyses are conducted prior to the system's dynamic analyses to obtain the system's natural periods. This analysis is conducted by coupling the AHSE component of the FOWT system in OpenFAST and then switching off the aerodynamic flag and the wave mode flag to ensure no aerodynamic load and wave load respectively. The platform is displaced from an assigned initial position in the required degree of freedom to determine the natural

period. For the purpose of this study, the Surge, Heave and Pitch DOF are assessed for the system's natural period. The corresponding initial displacement of the platform and estimated natural periods for each DOF considered for the three optimal platforms are shown in Table 13. In addition, the decay responses in the specified DOFs (heave pitch and surge) for the three optimal variants are shown in Fig. 12. The natural period in the heave DOF presented for the three optimal cases in Fig. 12 shows how the platform waterplane area geometry affects the system's natural period. The  $7^{\circ}$  static angle case has the lowest heave stiffness at the mean sea level (MSL) due to significantly small diameter of the control point at the water level. This leads to significant heave motion and natural period in this case in comparison to the other two cases (5° and  $10^{\circ}$  static angle variants) with larger diameter of the control points

**Table 13**Natural Period of optimal variants from free-decay test.

Optimal Case	Static Pitch Angle (Degrees)	Degree of Freedom	Initial Displacement	Natural Period (sec)
Case A	5	Surge	15 m	121
Case A	5	Heave	10 m	25
Case A	5	Pitch	5 deg	28
Case B	7	Surge	15 m	116
Case B	7	Heave	10 m	87
Case B	7	Pitch	5 deg	32
Case C	10	Surge	15 m	110
Case C	10	Heave	10 m	48
Case C	10	Pitch	5 deg	40

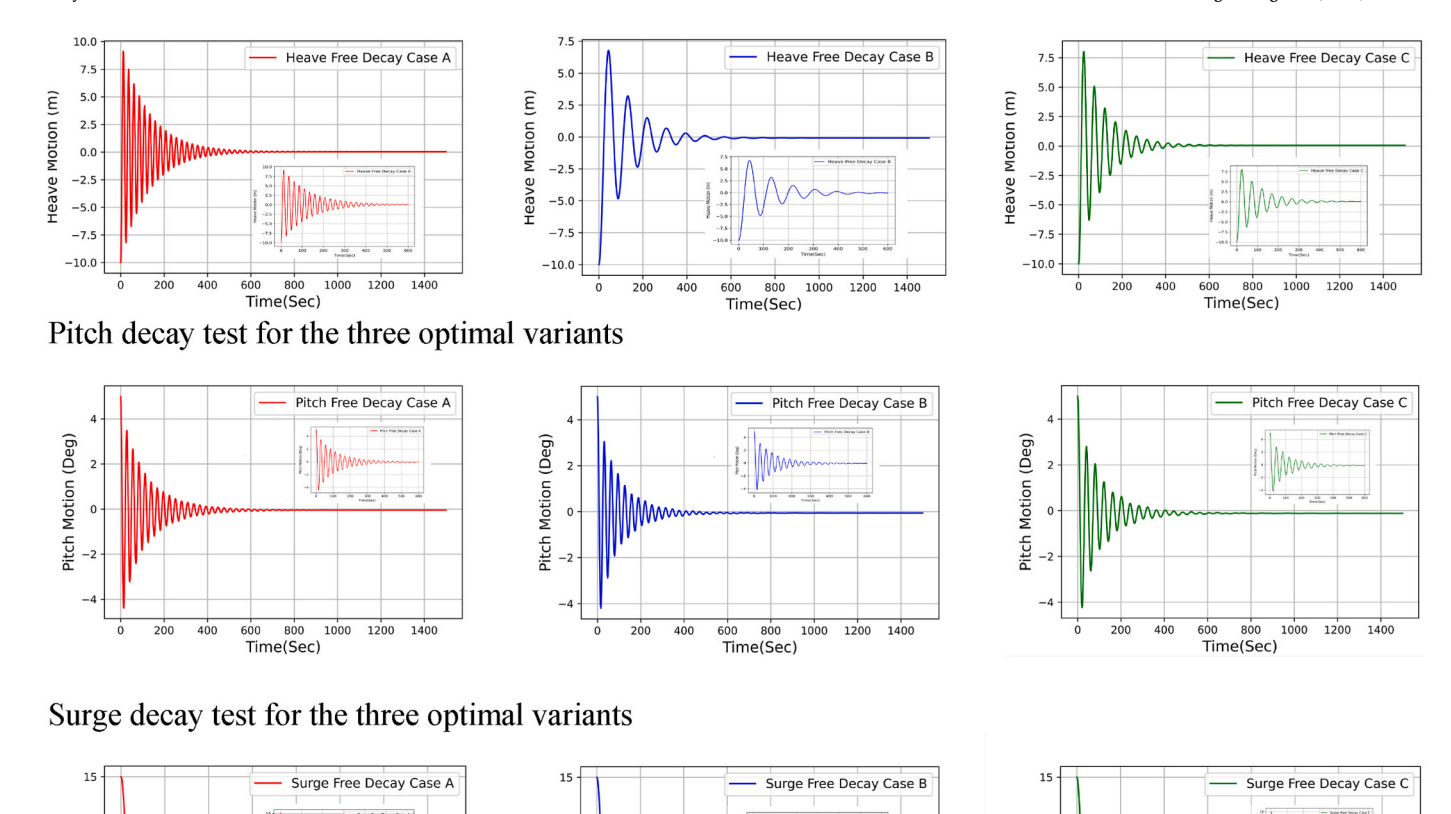


Fig. 12. Heave, Pitch and Surge decay test for the three optimal variants.

Time(Sec)

1000

Surge Motion (m)

at the MSL.

200 400

Surge Motion (m)

5.4.2.2. FOWT system dynamic response analysis -optimal variants. The dynamic analysis for this study is conducted according to the DLC1.6a load case from IEC-61400-3-2 (2019) considering severe sea state of 50 years return period. The corresponding sea state utilized is highlighted in Table 8 with a significant wave height of 10.37 m, peak period of 14.7 s at a rated wind speed of 12 m/s. The wind and wave loads are set to be colinear on the FOWT system along the surge DOF of the platform for conservative analysis. This simulation has been conducted for severe sea state requirements as highlighted in IEC-61400-3-2 (2019) and Jonkman (2007) in which a six 1-h simulations at each sea state and the simulations are differentiated by the wave seeds. The average of the simulations from the 6 wave seeds are plotted to determine the system's response as highlighted in Fig. 13. As highlighted in the global dynamic analysis in the frequency domain Section 5.4.1, Fig. 11, the system's RAO in all DOFs considered are well decoupled from the associated wave spectrum indicating a good design.

1000 1200

Time(Sec)

The platform motions in the 6 DOFs presented in Fig. 13 are estimated considering a simulated time of 3600 s. The platform motion in time domain showing the maximum, mean, minimum motion and standard deviation for the selected optimal cases in all DOFs is highlighted in Table 14 excluding the initial transient period of around 500 s of the simulation time.

Fig. 13 shows the platform response in surge DOF for the three optimal cases with Case C (10 deg static pitch angle) showing the largest

average displacement in surge of 24.79 m. The average displacement of 24.79 m shows the surge motion is still less than 15 % of the 320 m water depth which is the allowable translational motion benchmark set for this study. The most notable maximum mean heave displacement of all the three optimal cases is highlighted in Case B ( $-4.13\,\mathrm{m}$ ). This is due to the platform's shape at the waterplane area. A small diameter at the water plane area results in a reduction in the magnitude of the heave stiffness and a significant increase in the platform's heave motion and its natural period as highlighted in the heave free decay test in Fig. 12. For the pitch displacement, Case C (10 deg static pitch angle constraint) has the largest pitch displacement as it also has the largest static pitch angle of inclination constraint utilized for the optimization process in Section 4. This shows the platform's optimal shape from the optimization constraint is a huge contributory factor to the pitching displacement of the FOWT system.

200 400

1200

1000

Time(Sec)

Surge Motion (m)

5.4.2.3. Nacelle acceleration. A key global performance metric used in assessing the optimal design models is the nacelle acceleration RMS value. The FOWT system's nacelle acceleration allowable limit is less than 30 % of the acceleration due to gravity (g) (Leimeister et al., 2020b; Rasekhi Nejad et al., 2017). This is equivalent to values below 2.943 m/s². The statistics of the root mean square value of the nacelle acceleration is determined from the time signal of the nacelle acceleration in the three translational DOF is highlighted in Table 15 and Fig. 14.

From Table 15, Case A optimal variant has the largest RMS value for nacelle acceleration of  $0.31 \text{ m/s}^2$ . This RMS value of  $0.31 \text{ m/s}^2$  is still

Ocean Engineering 332 (2025) 121378

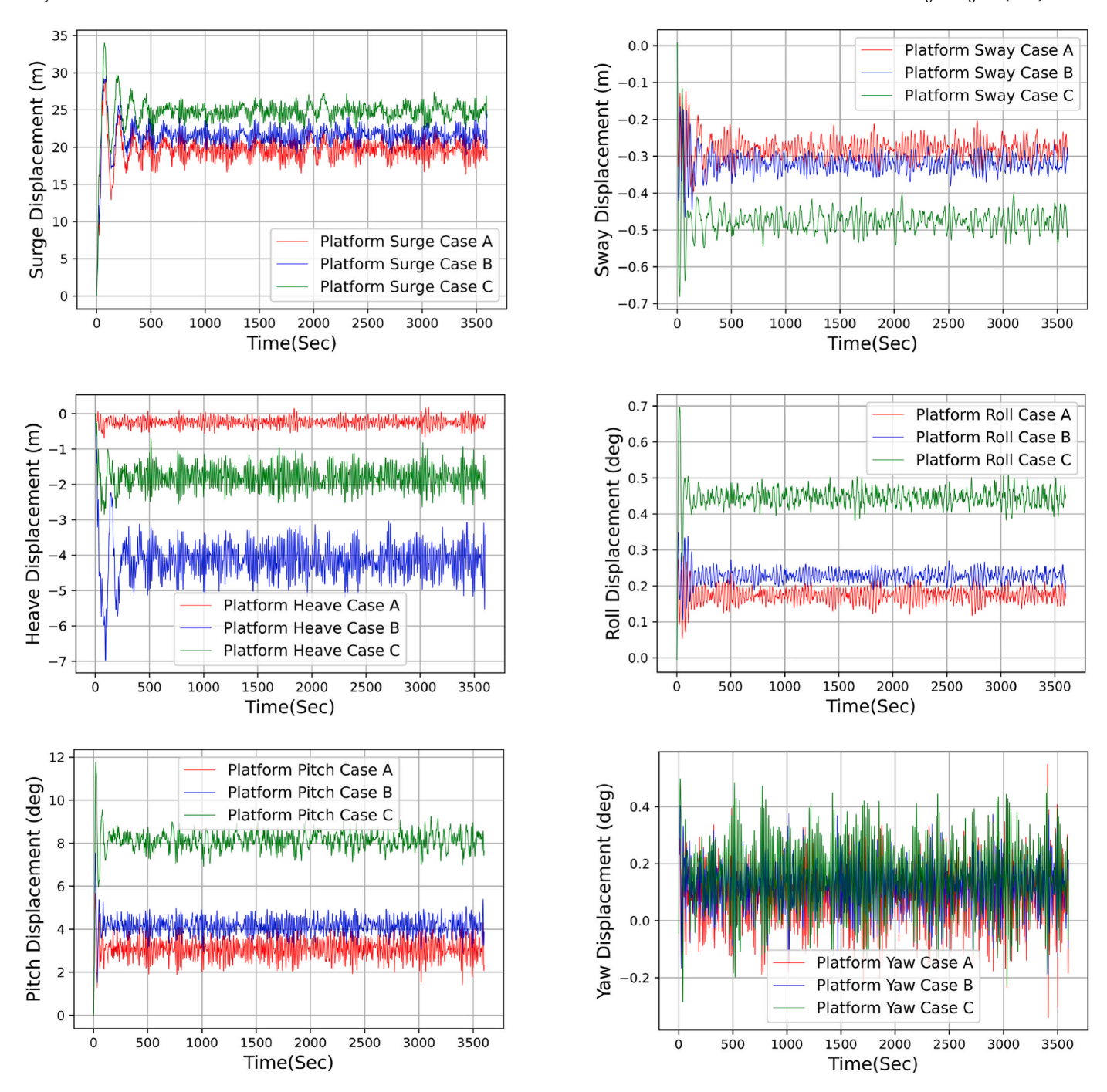


Fig. 13. Platform optimal variants coupled translational and rotational response.

within allowable limit of  $2.943~\text{m/s}^2$  highlighting the operational capability of the of the selected optimal design variants in severe sea states. As expected, the RNA fore-aft accelerations derived with the nonlinear, time-domain approach are higher than their counterparts derived with the frequency domain approach.

#### 5.4.3. Discussion

The parametric shape alteration and optimization design approach of a 5 MW spar FOWT platform developed in this study is a unique approach that can be extended to designing and scaling higher turbine nameplate capacity spar like  $10\,\mathrm{MW}$  or  $15\,\mathrm{MW}$ . As highlighted in review of literature conducted in Ojo et al. (2022a), this framework can be used to alter the shape of foundations of large turbines for material reduction and exploration of improved hydrodynamic response.

Mass reduction of platform and its hydrodynamic response requires a careful calibration to ensure a functional system. The key trade-offs between mass reduction and hydrodynamic performance in deep water involve balancing cost savings with stability, motion control, and structural resilience. While reducing mass has a strong potential to reduce manufacturing costs, it increases sensitivity to wave loads, mooring complexity, and fatigue risks. This framework employs a systematic approach that integrates a robust platform's shape alteration technique with the pattern search optimizers to mitigate the high sensitivity hydrodynamic risks of mass reduction while maintaining cost-effectiveness, stability, acceptable motion response, and long-term durability in deep-water applications.

The capability of the framework to select optimal platform shape altered variants that retains desired hydrodynamic properties and

**Table 14**Descriptive motion response statistics of optimal variants.

Optimal Cases	Static Pitch Angle (Degrees)	Degree of Freedom	Maximum	Mean	Minimum	Standard Deviation
Case A	5	Surge	22.77 m	19.62 m	16.36 m	1.05
Case A	5	Sway	-0.20  m	-0.28  m	−0.35 m	0.02
Case A	5	Heave	0.18 m	−0.24 m	−0.65 m	0.11
Case A	5	Roll	0.23 deg	0.17 deg	0.12 deg	0.02
Case A	5	Pitch	4.29 deg	3.07 deg	1.41 deg	0.42
Case A	5	Yaw	0.55 deg	0.09 deg	-0.34 deg	0.10
Case B	7	Surge	24.94 m	21.55 m	18.89 m	0.87
Case B	7	Sway	-0.27  m	-0.32  m	−0.38 m	0.02
Case B	7	Heave	-3.02  m	-4.13 m	−5.53 m	0.37
Case B	7	Roll	0.27 deg	0.23 deg	0.18 deg	0.01
Case B	7	Pitch	5.39 deg	4.14 deg	2.89 deg	0.34
Case B	7	Yaw	0.42 deg	0.12 deg	−0.19 deg	0.08
Case C	10	Surge	27.40 m	24.79 m	21.53 m	0.85
Case C	10	Sway	-0.40  m	-0.47  m	−0.54 m	0.02
Case C	10	Heave	-0.73  m	-1.79  m	-2.63 m	0.28
Case C	10	Roll	0.51 deg	0.45 deg	0.38 deg	0.02
Case C	10	Pitch	9.25 deg	8.12 deg	6.91 deg	0.37
Case C	10	Yaw	0.48 deg	0.16 deg	$-0.23 \deg$	0.11

 Table 15

 Nacelle acceleration statistics from time domain simulation.

	Case A (m/s <sup>2</sup> )	Case B (m/s <sup>2</sup> )	Case C (m/s <sup>2</sup> )
Nacelle Acceleration RMS	0.310	0.260	0.202

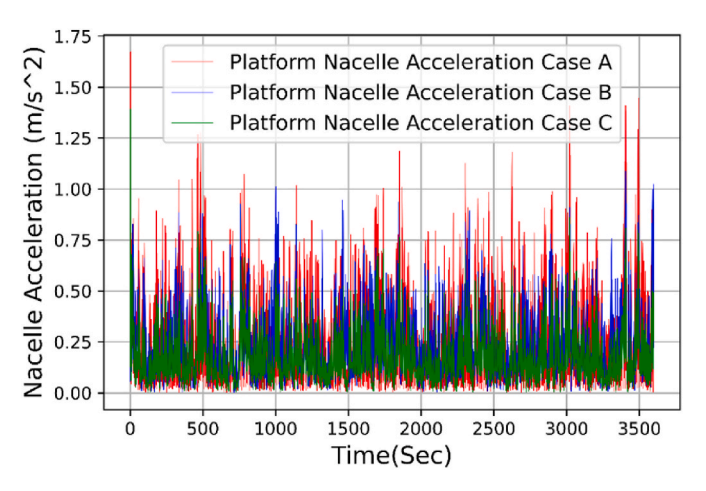


Fig. 14. Nacelle acceleration response spectrum from time domain simulation.

motion response with reduced mass is shown in the results highlighted in Table 13 – platform's natural period, Table 14 – motion response statistics under severe environmental loading and Table 15 – estimated nacelle acceleration. All the responses in Table 13, Tables 14 and 15 are within the allowable responses for a Spar type FOWT. Also, in normal operating condition shown in Table 6, the responses of the variant platforms are closely matched with the conventional designed OC3 Spar floating platform. It is worth noting that the developed framework, like other design processes involves complex risks that spans structural integrity, environmental impact, hydrodynamic stability and financial feasibility that must be mitigated with advanced monitoring, engineering innovation and a balanced multi-disciplinary risk management strategy. For example, a design and manufactured platform in operation is subjected to oscillatory motions induced by waves and current requiring adequate monitoring of the platform's structural health.

In addition to the shape alteration of a traditional ballast stabilised spar platform, this shape alteration design and optimization framework can be used in platform types like the water-plane stabilised semi-submersible and mooring stabilised TLP.

#### 6. Conclusion, limitation and recommendations

#### 6.1. Conclusion

It is a known consensus that the FOWT technology is not as competitive as its fixed bottom counterpart due to the substantial computational time and capital costs involved in design, analysis and manufacturing FOWT systems. This is partly due to the FOWT technology still being in the precommercial stage. Weight and cost reductions are key to the expected commercialization of FOWT system, as the platform's cost is currently 28.5 % of the FOWT's capital expenditure (CAPEX) cost. Commercializing the technology of floating offshore wind will require it being as competitive as the fixed bottom turbine technology and one way of addressing this is adapting the use of shape parameterization technique within an MDAO framework. This work highlights the utilization of parametric curves to alter the geometric shapes of a FOWT substructure/platform while simultaneously optimizing the FOWT system. The automatic numerical MDAO framework (implements automatic input of design variables) developed for this study employs the use of parametric curves (NURBS), structural, hydrostatics and hydrodynamic modelling and analysis tools in frequency domain (DNV suites) and optimizers (meta-heuristics) to estimate the system's fitness for purpose. The use of a NURBS approximation curve for modelling the spar platform of the FOWT system allows the geometric shape alteration as a result of the local propagation property along the control points on the NURBS curve. This capability is the core novelty of the present methodology, since it differs from previous work in this area, where a simpler approach consisting in changing only the diameters and height of a few cylindrical elements representing the platform was used - the present methodology therefore allows the exploration of richer design space for the selection of the optimal models. An important constraint utilized in the optimizers is the static pitch constraints for hydrostatic equilibrium. Static pitch angles of 5 deg, 7 deg and 10 deg are considered and for each pitch angle case, the MDAO framework cycles through an average of 2500 iterations to select the optimal design.

Verification of each of the optimal design is conducted with medium-fidelity OpenFAST time domain AHSE tool. The platform's frequency dependent damping and added mass data, the excitation force data and calculation of the heave, pitch and roll hydrostatic stiffnesses are coupled in OpenFAST. In addition to this, the platform's pitch, roll and yaw inertia are calculated for the optimal variants and coupled with the platform mass and centre of mass in the structural section of the AHSE tool and a dynamic analysis in a severe seastate is conducted while the FOWT system is operating at rated wind speed. The response and performance of the system's design variants at the rated wind speed are all

acceptable and within allowable limits from the design standards.

A key finding of this study shows that the steel mass needed for the manufacturing of a FOWT platform gets smaller as the static pitch angle of inclination increases from 5 deg, 7 deg, and 10 deg respectively, corresponding to Case A, Case B and Case C as highlighted in Table 9. This reduction in mass inherently translates to lower cost. In addition to reducing the steel mass for design and fabrication, bespoke geometric shapes of the platform that with acceptable hydrodynamic motion responses in severe seastates are generated. An important advantage of this MDAO framework with geometric alteration capability is that it can be applied to any design concept, optimally varying its shape, improving some of the key global response performance and aiming at reducing the structural weight, ultimately leading to a lower cost.

The main contribution of this study is the capability.

#### 6.2. Contribution and limitation

The primary contribution of this study is the systematic modelling of a spar platform using available tools, including NURBS and hydrodynamic tools – HydroD, WADAM integrated with a gradient free pattern search optimization algorithm to optimize its shape. This approach aims to reduce the capital cost of a FOWT while enhancing its hydrodynamic response. Furthermore, this systematic methodology can be extended to other floating platform types, such as semi-submersibles and Tension Leg Platforms. A Potential limiting factor of the concept proven in this study is the manufacturability of the bespoke geometric shapes from the framework. These bespoke shapes are complex and can pose potential difficulty in manufacturing. As highlighted in section 1.3, traditional or subtractive manufacturing processes often involve a significant amount of material waste for a simple design; hence, an increase in design complexity has the potential to substantially increase material waste and nullify the advantage of the concept described in this study. However, research in metal additive manufacturing techniques is gathering pace to address this issue. As highlighted in section 1.3, metal additive manufacturing techniques like direct energy deposition and Wire-arc have arrived at a developmental scale suitable for construction use to potentially provide reduced wastage of manufacturing materials while enhancing, automation and customization in manufacturing coupled with increased productivity.

# 6.3. Recommendations

This study has established the use of shape parameterization technique within an MDAO framework using commercially available software suite (DNV SESAM suite) and developed a glue code with the capability of integrating different disciplines and automating the search of a large design space. The current work can be especially useful for researchers and developers engaged in the conceptual development of floating platform because it offers insights on the optimal variants of different spar platform concepts. However, there is need for future work to enhance the research.

This framework can be extended to different platform types with different stability mechanisms like the semi-submersible and the TLP. This will enhance the design of the platform types as the various stability mechanisms contributing to the platform's stability requirements will be optimized in the design process.

This work has only looked at DLC 1.6a load case for a severe seastate with the view of assessing the response of the FOWT system in severe seastates and although, the global response of the optimal design variants are worse than the OC3 spar, they are all still within allowable limits as recommended in design standards (IEC-61400-3-2, 2019). It is recommended to subject optimal shape design to other load cases and a wide variety of constraints including structural integrity ones. Another recommendation is to conduct a detailed analysis on the optimal design variants i.e., conducting detailed structural assessment on the optimal platform by assessing the fatigue, serviceability, and ultimate limit

states. In addition, as manufacturability has been highlighted as a limitation of the design and optimization concept proven in this work, a review of the manufacturability of the optimal geometric shape variants using the new metal additive manufacturing technologies and concrete slip-forming of platforms should be explored to ensure there is adequate capability in producing physical components of the bespoke FOWT designs.

While steel has been used as the primary material for this study as weight optimization is a critical requirement in deep-water spar design, concrete material can be explored when durability, cost stability and corrosion resistance are requirements. However, due to the weight increase in concrete, it is recommended to use a hybrid of steel-concrete to design and optimize a composite spar to get the best properties from both materials.

The framework in this study is built around a single objective function which is the reduction in the mass of steel, potentially leading to capital cost reduction and in some cases improved hydrodynamic response. It is recommended to explore the use of multi-objective optimization function over a single objective function to allow for a simultaneous optimization of multiple conflicting objectives (mass of steel, system's hydrodynamic response, fatigue life and other functions) leading to a potentially more balanced and comprehensively informed decision-making process.

Although the key words in this study are parameterization and optimization within an MDAO framework, an interesting future work is the upscaling of an optimal model of a geometry parameterized platform with a larger turbine to satisfy the operational requirements of the larger turbine starting from the system's stability. Although research studies have been conducted on platform upscaling in other offshore sectors and the FOWT sector, upscaling an optimal shape parameterized platform with a larger turbine is a bespoke study recommended for research in the FOWT sector as it is anticipated highly enhance the commercial competitiveness of the FOWT technology against the fixed-bottom technology.

#### CRediT authorship contribution statement

Adebayo Ojo: Writing – original draft, Visualization, Validation, Software, Methodology, Investigation, Formal analysis, Data curation, Conceptualization. Maurizio Collu: Writing – review & editing, Validation, Supervision, Resources, Project administration, Methodology, Funding acquisition, Formal analysis, Conceptualization. Andrea Coraddu: Writing – review & editing, Supervision, Project administration, Investigation, Conceptualization.

#### **Declaration of competing interest**

The authors declare that they have no known competing financial interests or personal relationships that could have appeared to influence the work reported in this paper.

#### Acknowledgement

This work is conducted with the Renewable Energy Marine Structures (REMS) group at the University of Strathclyde and the funding is provided by the Engineering and Physical Sciences Research Council (EPSRC) UK (Grant no: EP/L016303/1).

#### References

Anaya-Lara, O., Tande, J.O., Uhlen, K., Merz, K., 2018. Offshore Wind Energy Technology. John Wiley & Sons.

Bachynski, E.E., Collu, M., 2019. Offshore support structure design. Renewable Energy from the Oceans: from Wave, Tidal and Gradient Systems to Offshore Wind and Solar. Institution of Engineering and Technology, pp. 271–319.

Bachynski, E.E., Moan, T., 2012. Design considerations for tension leg platform wind turbines. Mar. Struct. 29 (1), 89–114.

- Birk, L., 2006. Parametric modeling and shape optimization of offshore structures. Int. J. CAD/CAM 6 (1), 29–40.
- Butterfield, S., Musial, W., Jonkman, J.M., Sclavounos, P.D., 2007. Engineering Challenges for Floating Offshore Wind Turbines.
- Clauss, G.F., Birk, L., 1996. Hydrodynamic shape optimization of large offshore structures. Appl. Ocean Res. 18 (4), 157–171.
- Collu, M., Borg, M., 2016. Design of Floating Offshore Wind Turbines, Offshore Wind Farms: Technologies, Design and Operation. Elsevier Inc., pp. 359–385
- Cordle, A., Jonkman, J.M., 2011. State of the Art in Floating Wind Turbine Design Tools. DNV, 2021. Sesam feature description. Software Suite for Hydrodynamic and Structural Analysis of Renewable, Offshore and Maritime Structures. DNV.
- DNVGL Høvik, N., 2019. SESAM User Manual, WADAM, Wave Analysis by Diffraction and Morison Theory.
- DNVGL Oslo, N., 2018. Class Guideline DNVGL CG 0130: Wave Loads.
- ElMaraghy, W., ElMaraghy, H., Tomiyama, T., Monostori, L., 2012. Complexity in engineering design and manufacturing. CIRP Ann. 61 (2), 793–814.
- Farin, G., 1990. Curves and Surfaces for Computer-Aided Geometric Design. Academic Press, New York.
- Findler, N.V., Lo, C., Lo, R., 1987. Pattern search for optimization. Math. Comput. Simulat. 29 (1), 41–50.
- Frank Lemmer, K.M., Yu, Wei, Ricardo Faerron Guzman, M.K., 2016. Life50+:- D4.3 Optimization Framework and Methodology for Optimized Floater Design.
- Fylling, I., Berthelsen, P.A., 2011. WINDOPT: an optimization tool for floating support structures for deep water wind turbines, volume 5: ocean space utilization. Ocean Renew. Energy 767–776.
- Gardner, L., 2023. Metal additive manufacturing in structural engineering review, advances, opportunities and outlook. Structures 47, 2178–2193.
- Hall, M., Buckham, B., Crawford, C., 2013. Evolving offshore wind: a genetic algorithmbased support structure optimization framework for floating wind turbines, OCEANS 2013 MTS/IEEE Bergen: the challenges of the Northern Dimension. IEEE 1–10.
- He, J., Jin, X., Xie, S.Y., Cao, L., Lin, Y., Wang, N., 2019. Multi-body dynamics modeling and TMD optimization based on the improved AFSA for floating wind turbines. Renew. Energy 141, 305–321.
- Hegseth, J.M., Bachynski, E.E., Martins, J.R., 2020. Integrated design optimization of spar floating wind turbines. Mar. Struct. 72, 102771.
- Hirai, T., Sou, A., Nihei, Y., 2018. Wave load acting on advanced spar in regular waves. In: Int. Conf. Offshore Mech and Arctic Eng. OMAE2018-77821, V006T05A024, p. 8.
- IEC61400-3-1, 2019. Wind Energy Generation Systems Part 3-1: Design Requirements for Fixed Offshore Wind Turbines.
- ${\tt IEC-61400-3-2,\ 2019.\ Wind\ Energy\ Generation\ Systems-Part\ 3-2:\ Design\ Requirements}$  for Floating Offshore Wind Turbines.
- Ioannou, A., Liang, Y., Jalón, M.L., Brennan, F.P., 2020. A preliminary parametric techno-economic study of offshore wind floater concepts. Ocean Eng. 197, 106937.
  Jonkman, J., Butterfield, S., Musial, W., Scott, G., 2009. Definition of a 5-MW Reference
- Jonkman, J., Butterfield, S., Musial, W., Scott, G., 2009. Definition of a 5-MW Reference Wind Turbine for Offshore System Development. National Renewable Energy Lab. (NREL), Golden, CO (United States).
- Jonkman, J.M., 2007. Dynamics Modeling and Loads Analysis of an Offshore Floating Wind Turbine. University of Colorado at Boulder.
- Jonkman, J.M., 2010. Definition of the Floating System for Phase IV of OC3.
- Journée, J.M.J., Massie, W.W., 2000. Offshore Hydromechanics, first ed. Delft University of Technology.
- Karimi, M., 2018. Frequency Domain Modeling and Multidisciplinary Design
   Optimization of Floating Offshore Wind Turbines. University of Victoria.
   Karimi, M., Buckham, B., Crawford, C., 2019. A fully coupled frequency domain model
- Karimi, M., Buckham, B., Crawford, C., 2019. A fully coupled frequency domain mode for floating offshore wind turbines. J. Ocean Eng. Marine Energy 5 (2), 135–158.
   Karimi, M., Hall, M., Buckham, B., Crawford, C., 2017. A multi-objective design
- Karimi, M., Hall, M., Buckham, B., Crawford, C., 2017. A multi-objective design optimization approach for floating offshore wind turbine support structures. J. Ocean Eng. Marine Energy 3 (1), 69–87.
- Kochenderfer, M.J., Wheeler, T.A., 2019. Algorithms for Optimization. Mit Press. Kolios, A., Borg, M., Hanak, D., 2015. Reliability analysis of complex limit states of floating wind turbines. J. Energy Chall. Mech. 2 (1), 6–9.
- Kolja Müller, D.M., Karch, Michael, Simon Tiedemann, R.P., 2017. Life50+: D7.5 Guidance on Platform and Mooring Line Selection, Installation and Marine Operations.

- Laguna, M., Martí, R.C., 2003. Scatter Search: Methodology and Implementations in C. Springer Science & Business Media.
- Leimeister, M., Collu, M., Kolios, A., 2022. A fully integrated optimization framework for designing a complex geometry offshore wind turbine spar-type floating support structure. Wind Energ. Sci. 7 (1), 259–281.
- Leimeister, M., Kolios, A., Collu, M., 2018. Critical review of floating support structures for offshore wind farm deployment. J. Phys. Conf. 1–11.
- Leimeister, M., Kolios, A., Collu, M., 2020a. Development and verification of an aero-hydro-servo-elastic coupled model of dynamics for FOWT. Based MoWiT Library 13 (8), 1974.
- Leimeister, M., Kolios, A., Collu, M., Thomas, P., 2020b. Design optimization of the OC3 phase IV floating spar-buoy, based on global limit states. Ocean Eng. 202, 107186. MathWorks, 2021. MATLAB Global Optimization Toolbox - Pattern Search.
- Newman, J.N., 2018. Marine Hydrodynamics. The MIT press.
- Ojo, A., Collu, M., Coraddu, A., 2022a. Multidisciplinary design analysis and optimization of floating offshore wind turbine substructures: a review. Ocean Eng. 266, 112727.
- Ojo, A., Collu, M., Coraddu, A., 2022b. Parametrisation scheme for multidisciplinary design analysis and optimisation of a floating offshore wind turbine substructure – OC3 5MW case study. J. Phys. Conf. 2265 (4), 042009.
- OpenFAST, 2023. Openfast Documentation.
- Palacio-Morales, J., Tobón, A., Herrera, J., 2021. Optimization based on pattern search algorithm applied to pH non-linear control: Application to alkalinization process of sugar juice. Processes 9 (12), 2283.
- Patel, M.H., 2013. Dynamics of Offshore Structures. Butterworth-Heinemann.
- Pham, T.D., Shin, H., 2019. A new conceptual design and dynamic analysis of a spar-type offshore wind turbine combined with a moonpool. Energies 12 (19).
- Qiu, C., Tan, J., Liu, Z., Mao, H., Hu, W., 2022. Design theory and method of complex products: a review. Chin. J. Mech. Eng. 35 (1), 103.
- Rasekhi Nejad, A., Bachynski, E.E., Moan, T., 2017. On Tower Top Axial Acceleration and Drivetrain Responses in a Spar-type Floating Wind Turbine.
- Saenz-Aguirre, A., Ulazia, A., Ibarra-Berastegi, G., Saenz, J., 2022. Floating wind turbine energy and fatigue loads estimation according to climate period scaled wind and waves. Energy Convers. Manag. 271, 116303.
- Samareh, J.A., 2001. Survey of shape parameterization techniques for high-fidelity multidisciplinary shape optimization. AIAA J. 39 (5), 877–884.
- Sandner, F., Wie, F.Y., Matha, D., Grela, E., Azcona, J., Munduate, X., Voutsinas, S., Natarajan, A., 2014. Deliverable D4. 33—Innovative concepts for floating structures. InnWind. EU 10. 11–31.
- Siemens, 2009. Siemens Wind Turbine SWT-2.3-82 VS, Technical Brochure.
- Torczon, V., Trosset, M.W., 1998. From evolutionary operation to parallel direct search: pattern search algorithms for numerical optimization, computing science and statistics. Citeseer 396–401.
- Tracy, C.H., 2007. Parametric Design of Floating Wind Turbines. Massachusetts Institute of Technology.
- Tyler, S., Patrick, D., 2022. 2021 Cost of Wind Energy Review. National Renewable Energy Laboratory.
- Wayman, E.N., 2006. Coupled Dynamics and Economic Analysis of Floating Wind Turbine Systems. Massachusetts Institute of Technology.
- Wolpert, D.H., Macready, W.G., 1997. No free lunch theorems for optimization. IEEE Trans. Evol. Comput. 1 (1), 67–82.
- Wright, C., Yoshimoto, H., Wada, R., Takagi, K., 2019, June. Numerical modelling of a relatively small floating body's wave and low frequency motion response, compared with observational data. In: *International Conference on Offshore Mechanics and Arctic Engineering*, Vol. 58882. American Society of Mechanical Engineers.
- Yamanaka, S., Hirai, T., Nihei, Y., Sou, A., 2017, June. Interaction between advanced spar and regular waves. In: *International Conference on Offshore Mechanics and Arctic Engineering*, Vol. 57724. American Society of Mechanical Engineers.
- Yang, X.-S., 2019. 3 optimization algorithms. In: Yang, X.-S. (Ed.), Introduction to Algorithms for Data Mining and Machine Learning. Academic Press, pp. 45–65.
- Yoshimoto, H., Kamizawa, K., 2019. Validation of the Motion Analysis Method of Floating Offshore Wind Turbines Using Observation Data Acquired by Full Scale Demonstration Project.
- Zhu, H., Sueyoshi, M., Hu, C., Yoshida, S., 2019. A study on a floating type shrouded wind turbine: design, modeling and analysis. Renew. Energy 134, 1099–1113.